

Mol 45203

Partial deletion of the nicotinic cholinergic receptor $\alpha 4$ or $\beta 2$ subunit genes changes the acetylcholine sensitivity of receptor mediated $^{86}\text{Rb}^+$ efflux in cortex and thalamus and alters relative expression of $\alpha 4$ and $\beta 2$ subunits

Cecilia Gotti, Milena Moretti, Natalie M. Meinerz, Francesco Clementi, Annalisa Gaimarri, Allan C. Collins and Michael J. Marks

CNR, Institute of Neuroscience, Cellular and Molecular Pharmacology, Department of Medical Pharmacology and Center of Excellence on Neurodegenerative Diseases, University of Milan, Milan, Italy (CG, MM, FC, AG) and Institute for Behavioral Genetics, University of Colorado, Boulder, Colorado, USA (NMM, ACC, MJM)

Mol 45203

Running title: Partial gene deletion and nicotine receptor expression

Corresponding author

Michael Marks

Institute for Behavioral Genetics, 447 UCB

University of Colorado, Boulder

1480 30th St.

Boulder, Co 80303

Phone: 1.303.492.9677

Fax: 1.303.492.8063

E-mail: marksm@colorado.edu

Number of text pages: 48

Number of tables: 1

Number of Figures: 10

Number of references: 40

Words in Abstract: 244

Words in Introduction: 744

Words in Discussion: 1430

Abbreviations: nAChR, nicotinic acetylcholine receptor; A85380, 3-((2S)-azetidylmethoxy)pyridine; α Bgtx, α Bungarotoxin; PMSF, phenylmethanesulfonyl fluoride; Ab, polyclonal antibody.

Abstract

$\alpha 4$ and $\beta 2$ nicotinic cholinergic receptor (nAChR) subunits can assemble in heterologous expression systems as pentameric receptors with different subunit stoichiometries that exhibit differential sensitivity to activation by acetylcholine yielding biphasic concentration-effect curves. nAChR-mediated $^{86}\text{Rb}^+$ efflux in mouse brain synaptosomes also displays biphasic ACh concentration-response curves. Both phases are mediated primarily by $\alpha 4\beta 2^*$ -nAChR, since deletion of either the $\alpha 4$ or $\beta 2$ subunit reduces response at least 90%. A relatively larger decrease in the component of $^{86}\text{Rb}^+$ efflux with lower ACh sensitivity occurred with partial deletion of $\alpha 4$ ($\alpha 4^{+/-}$) whereas a larger decrease in the component with higher ACh sensitivity was elicited by partial deletion of $\beta 2$ ($\beta 2^{+/-}$).

Immunoprecipitation with selective antibodies demonstrated that more than 70% of [^3H]-epibatidine binding sites in both regions contained only $\alpha 4$ and $\beta 2$ subunits. Subsequently, $\alpha 4$ and $\beta 2$ subunit content in the cortex and thalamus of $\alpha 4$ and $\beta 2$ wild-types and heterozygotes was analyzed with Western blots. Partial deletion of $\alpha 4$ decreased and partial deletion of $\beta 2$ increased the relative proportion of the $\alpha 4$ subunit in assembled receptors. While these methods do not allow exact identification of stoichiometry of the subtypes present in wild-type cortex and thalamus, they do demonstrate that cortical and thalamic nAChRs of the $\alpha 4^{+/-}$ and $\beta 2^{+/-}$ genotypes differ in relative expression of $\alpha 4$ and $\beta 2$ subunits a result that corresponds to the relative functional changes observed following partial gene deletion. These results strongly suggest that $\alpha 4\beta 2$ -nAChR with different stoichiometry are expressed in native tissue.

Introduction

Nicotinic cholinergic receptors (nAChR) are a diverse family of ligand gated ion channels. Many receptor subunits are expressed in the brain and can assemble to form heteropentamers ($\alpha 2$, $\alpha 3$, $\alpha 4$, $\alpha 6$, $\beta 2$, $\beta 4$, $\alpha 5$, and $\beta 3$) or homopentamers ($\alpha 7$) (Lindstrom, 2000). Although many nAChR subtypes have been identified in the brain (Gotti et al., 2006), the most abundant subtype comprising binding sites measured with the promiscuous ligand, epibatidine (Badio and Daly, 1994; Houghtling et al., 1995; Davila-Garcia et al., 1997; Marks et al., 1998), are $\alpha 4\beta 2^*$ -nAChR (Zoli et al., 1998;; Ross et al., 2000; Marks et al., 2006, 2007). The $\alpha 4\beta 2^*$ -nAChR subtype is also the primary site measured by high affinity [^3H]-cytisine or [^3H]-nicotine binding (Whiting and Lindstrom, 1988; Flores et al., 1992; Picciotto et al., 1995; Marubio et al., 1999).

Since nAChR are pentameric, the possibility for molecular diversity is substantial. Even within a given subtype, the ratio of subunits assembled in the mature receptor could generate molecular subtypes with distinct physiology and pharmacology. Initial experiments examining heterologously expressed $\alpha 4\beta 2$ -nAChR with high sensitivity to activation by ACh, determined a likely stoichiometry of $(\alpha 4)_2(\beta 2)_3$ (Anand et al., 1991; Cooper et al., 1991). Subsequently, biphasic ACh concentration-effect curves for $\alpha 4\beta 2$ -nAChR have been observed in heterologous expression systems (Zwart and Vijverberg, 1998; Covernton and Connolly, 2000; Buisson and Bertrand, 2001; Nelson et al., 2003). Varying the ratio of $\alpha 4$ to $\beta 2$ altered agonist sensitivity ((Zwart and Vijverberg, 1998; Nelson et al., 2003; Khiroug et al., 2004; Moroni et al., 2006). Cells receiving excess $\beta 2$ subunits displayed higher sensitivity to ACh ($\text{EC}_{50} \approx 1 \mu\text{M}$) and those receiving excess $\alpha 4$ subunits displayed lower sensitivity ($\text{EC}_{50} \approx 100 \mu\text{M}$). The difference in ACh sensitivity has been attributed to the assembly of $\alpha 4\beta 2$ -nAChR with different α/β

stoichiometry. Indeed, injecting mRNA encoding linked $\alpha 4\beta 2$ subunits with either mRNA encoding $\beta 2$ or $\alpha 4$ generated ACh concentration effect curves displaying higher or lower ACh sensitivity, respectively (Zhou et al., 2003). These results strongly support the hypothesis that variation in α/β stoichiometry determines relative sensitivity to agonist activation in heterologous expression systems.

Several physiological and biochemical assays for nAChR function in brain preparations have been developed. Included in these is agonist-stimulated $^{86}\text{Rb}^+$ efflux (Marks et al., 1999). Biphasic ACh concentration-effect curves for stimulation of $^{86}\text{Rb}^+$ efflux from mouse brain synaptosomes, with EC_{50} values comparable to those in the heterologous systems, were observed (Marks et al., 1999). Although this assay could be measuring several receptor subtypes, deletion of either $\alpha 4$ (Marks et al., 2007) or $\beta 2$ (Marks et al., 1999, 2000) eliminated virtually all agonist-stimulated $^{86}\text{Rb}^+$ efflux in most brain regions establishing that most $^{86}\text{Rb}^+$ efflux is mediated by $\alpha 4\beta 2^*$ -nAChR. The molecular basis for the differential agonist sensitivity observed in native tissues may result from expression of $\alpha 4\beta 2^*$ -nAChR that differ in α/β stoichiometry as is the case with heterologous expression systems. Consequently, nAChR function could be regulated by differences in relative expression of α and β subunits resulting in altered sensitivity not only in normal activity, but also in response to nicotinic drugs (Marks et al., 1999; Moroni et al., 2006).

The demonstration that $^{86}\text{Rb}^+$ efflux and radiolabeled epibatidine binding in most brain regions is mediated by $\alpha 4\beta 2^*$ -nAChR is the basis for the series of studies described here. The approach applied to manipulate gene expression *in vivo* uses mice that have altered expression of $\alpha 4$ and $\beta 2$ achieved by the partial gene deletion obtained with heterozygous mutant mice ($\alpha 4^{+/-}$ and $\beta 2^{+/-}$). Partial or complete deletion of the $\alpha 4$ gene has no effect on the expression of $\beta 2$

Mol 45203

mRNA and partial or complete deletion of the $\beta 2$ gene has no effect on the expression of $\alpha 4$ mRNA. However, widespread decrease in the immunoreactivity for both subunits (Whiteaker et al., 2006) as well as a substantial decrease in radiolabeled epibatidine binding (Marks et al., 1999, 2000, 2006, 2007) was observed following partial or complete deletion of either the $\alpha 4$ or $\beta 2$ gene. Therefore, to examine whether changes in relative expression of $\alpha 4$ or $\beta 2$ genes affects nAChR expression, we have measured ligand binding and ACh-stimulated $^{86}\text{Rb}^+$ efflux in cortical and thalamic synaptosomes. Furthermore, the composition of the assembled receptors was examined by immunoprecipitation using a well characterized panel of subunit specific antibodies (Gotti et al., 2005 a, b; Moretti et al 2004) and by Western blotting using these same antibodies to measure the relative amounts of $\alpha 4$ and $\beta 2$ subunit protein in assembled receptors in wild-type mice and mice heterozygotic for $\alpha 4$ ($\alpha 4^{+/-}$) and $\beta 2$ ($\beta 2^{+/-}$) subunit expression.

Mol 45203

Materials and Methods.

Materials

(+/-)[³H]-Epibatine (specific activity = 70.6 Ci/mmol), [¹²⁵I]-A85380 (specific activity= 2200 Ci/mmol), ⁸⁶RbCl (initial specific activity=9-18 Ci/mg) and Optiphase Supermix scintillation cocktail were purchased from PerkinElmer Life and Analytical Sciences, Boston, MA, USA; [¹²⁵I]- α Bungarotoxin (α Bgtx); specific activity=220 Ci/mmol) was purchased from GE Healthcare (Piscataway, NJ, USA). Sucrose and HEPES, hemisodium salt were obtained from Roche Diagnostics, Indianapolis, IN, USA. Non-radioactive epibatidine, acetylcholine iodide, diisopropylfluorophosphate, phenylmethylsulfonylfluoride (PMSF), EDTA, EGTA, bovine serum albumin, atropine sulfate, acetylcholine iodide, tetrodotoxin, TRIS, triton X-100, Tween-20, glucose, nicotine sulfate, NaCl, KCl, MgSO₄, CaCl₂ and polyethylenimine were purchased from Sigma, St. Louis, MO, USA. CsCl was obtained from RPI, Mt. Prospect, IL, USA.

Mice.

Animal care and experimental procedures were approved by the University of Colorado Animal Care and Utilization Committee.

Mice engineered by homologous recombination to express null mutation of the α 4 nAChR subunit (Ross, et al 2000) were originally obtained from the Howard Florey Institute, The University of Melbourne, Victoria, Australia. Mice engineered to express the null mutation for the β 2 subunit (Picciotto et al., 1995) were originally obtained from Yale University, New Haven, CT, USA. Mice used in these studies were maintained at the Institute for Behavioral Genetics, University of Colorado, Boulder, CO, USA in a vivarium maintained at 22 \pm 1°C with lights on between 7 AM and 7 PM. The α 4 mice had been backcrossed with C57BL/6 mice for

Mol 45203

two generations and the $\beta 2$ mice had been backcrossed with C57BL/6 mice for ten generations at the time of experimentation. All animals were produced by mating mice that were heterozygous for the appropriate mutation. Animals were weaned when 25 days old and subsequently housed with like-sexed littermates. All mice were allowed free access to food (Harlan Teklad, Madison, WI, USA) and water.

Genotypes were determined using DNA extracted from tail clippings obtained around 40 days of age as described previously (Salminen et al., 2004). Animals were 60-120 days old when used.

Tissue preparation.

Each mouse was killed by cervical dislocation. The brain was removed, placed on an ice-cold platform and the cerebral cortex and thalamus were dissected. Tissue samples to be used for functional assays were placed in ice-cold 0.32 M sucrose, buffered to pH 7.5 with 5 mM HEPES hemisodium. Tissue samples to be used for immunochemical studies were rapidly frozen on dry ice.

Crude synaptosomal preparation.

Cortical and thalamic tissue was homogenized by hand in 10 volumes of the 0.32 M sucrose/HEPES buffer using a glass-teflon tissue grinder. The subsequent homogenates were centrifuged at 12,000 x g for 20 min. The resulting crude synaptosomal pellets were suspended in isotonic uptake buffer (NaCl, 140 mM; KCl, 1.5 mM; MgSO₄, 1 mM; CaCl₂, 2 mM; glucose 20 mM; HEPES hemisodium salt, 25 mM; pH, 7.5). Cortical samples were suspended in 800 μ L and thalamic samples in 350 μ L.

⁸⁶Rb⁺ uptake.

Mol 45203

Twenty-five μL aliquots of synaptosomal suspension were added to 10 μL of uptake buffer containing approximately 4 μCi of $^{86}\text{Rb}^+\text{Cl}$. Samples were incubated for 30 min at 22°C at which time 5 μL of 80 μM diisopropylfluorophosphate was added to inhibit the acetylcholinesterase and samples were incubated an additional 5 min. Uptake was terminated and synaptosomes collected by filtration onto A/E glass fiber filters (Gelman, Ann Arbor, MI) under gentle vacuum (0.8 atm). Filters containing the synaptosomes were then washed with 0.5 mL of uptake buffer.

ACh-stimulated $^{86}\text{Rb}^+$ efflux.

Filters with the synaptosomes loaded with $^{86}\text{Rb}^+$ were placed on an open-air platform and superfused at 22°C with buffer (NaCl, 135 mM; KCl, 1.5 mM; CsCl, 5 mM; CaCl_2 , 2 mM; MgSO_4 , 1 mM; glucose, 20 mM; atropine, 1 μM ; tetrodotoxin, 50 nM; bovine serum albumin, 0.1%; HEPES hemisodium, 25 mM; pH, 7.5). Buffer was applied to the top of the filter with a Gilson Minipuls 3 peristaltic pump (Gilson, Middleton, WI, USA) at a rate of 2.5 ml/min and removed from the bottom of the filter with a second peristaltic pump set to a faster rate of 3.2 ml/min to actively remove buffer and prevent pooling. The effluent was pumped through a 200 μL Cerenkov cell in a β -Ram HPLC detector (IN/US Systems, Tampa, FL, USA) to monitor radioactivity continuously.

Samples were superfused for 5 min to allow basal efflux to stabilize before beginning data collection. Concentration-effect curves were constructed by exposing each filter to a single concentration of ACh (0.1 to 1000 μM) for 5 sec. A complete concentration-effect curve was constructed for both brain regions from each mouse assayed.

[^{125}I]-A85380 binding.

Mol 45203

Synaptosomes remaining after the measurement of $^{86}\text{Rb}^+$ efflux were diluted in 0.1 x uptake buffer and centrifuged at 12,000 x g for 15 min. The resulting pellet was suspended in the hypotonic buffer and centrifuged three additional times. The resulting sample was used to measure [^{125}I]-A85380 binding (Mukhin et al., 2000). Membranes were incubated at 22°C for 2 hr with one of eight concentrations of [^{125}I]-A85380 (between 2.0 pM and 300 pM) in a final volume of 30 μL of uptake buffer minus glucose. Inclusion of 100 μM cytosine established the blank. Binding was terminated by filtration onto GF/B glass fiber filter treated with 0.5% polyethylenimine in a 96-well plate (Unifilter, Whatman, Clifton, NJ, USA) using an Inotech Cell harvester (Inotech Biosystems, Rockville, MD, USA). Filters were subsequently washed 5 times with ice-cold buffer. Radioactivity was measured using a Wallac 1450 Microbeta scintillation counter (Perkin-Elmer Shelton, CT, USA) following addition of 50 μL of Optiphase Supermix scintillation cocktail to each well of the 96-well counting plate. Protein was measured by the method of Lowry et al. (1951) using bovine serum albumin as the standard.

Antibody production and characterization

The subunit-specific polyclonal antibodies (Abs) used were produced in rabbit against peptides derived from the C-terminal (COOH) or intracytoplasmic loop (Cyt) regions of rat (R), human (H) or mouse (M) subunit sequences and affinity purified as previously described (Zoli et al 2002). Most of the Abs have been previously described (Zoli et al 2002, Champtiaux et al 2003, Moretti et al 2004, Gotti et al . 2005 a, b).

Antibody specificity was checked by means of quantitative immunoprecipitation or immunopurification experiments using nAChRs from different areas of the CNS of wild- type and null mutant mice, which allowed selection of Abs specific for the subunit of interest, and established the immunoprecipitation capacity of each Ab (Zoli *et al.* 2002; Champtiaux *et al.*

Mol 45203

2003; Moretti et al 2004). Ab specificity was also tested by Western blotting, which showed that some of the Abs were less specific than in the immunoprecipitation experiments. Frequent monitoring of Ab properties is required because specificity is not only sequence related (the same peptide can be used to raise Abs with different degrees of specificity in different rabbits), but can also change over time in the same rabbit.

Preparation of cortex and thalamus membranes and 2% Triton X-100 extracts from $\alpha 4$ or $\beta 2$ genotypes

The cortex and thalamus were dissected, immediately frozen on dry ice, and stored at -80°C for later use. In every experiment, the tissues from cortex (0.3 -0.35 g) or thalamus (0.1 - 0.15 g) were homogenized in an excess (10 ml) of buffer (Na phosphate, 50 mM, pH 7.4; NaCl, 1 M; EDTA, 2 mM; EGTA, 2 mM and PMSF, 2 mM) for 2 min in an UltraTurrax homogenizer. The homogenates were then diluted and centrifuged for 1.5 h at 60,000xg. The 2% Triton X-100 extracts were prepared as previously described (Gotti et al 2005a,b). Protein content of the membranes, 2% Triton X-100 extracts and concentrated gradient fractions (see below) was measured using the bicinchonic acid protein assay (Pierce, Rockford, IL, USA) with bovine serum albumin as the standard.

[^3H]-Epibatidine binding.

In order to ensure that the $\alpha 7$ -containing subtypes did not contribute to [^3H]-epibatidine binding (Marks et al. 2006), both in membrane as well as in solubilized receptors (present in the extract and immunoprecipitation experiments) the binding were performed in the presence of 2 μM αBgtx , which specifically binds to $\alpha 7^*$ -nAChR (and thus prevents [^3H]-epibatidine binding to these sites).

Mol 45203

Membrane

Binding to the homogenates obtained from cortical or thalamic membranes was carried out overnight by incubating aliquots of the membrane with 2 nM [3 H]-epibatidine at 4°C. Non-specific binding (averaging 5-10% of total binding) was determined in parallel samples containing 100 nM unlabelled epibatidine.

At the end of the incubation, the samples were filtered on a GFC filter soaked in 0.5% polyethylenimine, washed with 15 ml of buffer (Na phosphate, 10 mM, pH 7.4; NaCl, 50 mM) and counted in a β counter.

Solubilized receptor

The Triton X-100 extracts, were labeled with 2 nM [3 H]-epibatidine. Tissue extract binding was performed using DE52 ion-exchange resin (Whatman, Maidstone, Kent,UK) as previously described (Vailati *et al.*, 1999).

Immunoprecipitation of [3 H]-epibatidine-labeled cortical receptors by anti-subunit-specific antibodies

The extracts (100-150 μ l) obtained from cortical and thalamic tissues of mice differing in $\alpha 4$ and $\beta 2$ genotypes were labeled with 2 nM 3 H-Epi, and incubated overnight with a saturating concentration of anti-subunit affinity-purified IgG (anti- $\alpha 2$, - $\alpha 3$, - $\alpha 4$, - $\alpha 5$, - $\alpha 6$, - $\beta 2$, - $\beta 3$ or - $\beta 4$). Each immunoprecipitate was recovered by incubating the samples with beads containing bound anti-rabbit goat IgG (Technogenetics, Milan, Italy). The level of immunoprecipitation with each Ab was expressed as the percentage of [3 H]-epibatidine-labeled receptors immunoprecipitated by the Abs (taking the amount present in the Triton X-100 extract solution before immunoprecipitation as 100%) or as fmol of immunoprecipitated receptors/mg of protein.

$\alpha 4\beta 2$ subtype immunopurification and analysis

The extracts prepared from mouse cortex ($\beta 2^{+/+}$) were incubated twice with 5 ml of Sepharose-4B and bound anti- $\beta 2$ Abs in order to remove the $\beta 2$ receptors from the extract. The bound $\beta 2^*$ -nAChRs were subsequently eluted from the Sepharose-4B with 0.2 M glycine, pH 2.2 or by competition with 100 μ M of the corresponding $\beta 2$ peptide used for Ab production.

The subunit content of the purified receptors was determined by immunoprecipitation using the purified subtypes eluted with the peptides labeled with 2 nM ^3H -Epi and the subunit specific antibodies .

Sucrose gradient centrifugation

In order to analyze the subunit stoichiometry of the nAChR subtypes, we used 5-20% sucrose gradients to separate the assembled nAChRs from the unassembled subunits present in the different genotypes.

To this end, linear 5-20% sucrose gradients in phosphate buffered saline plus 1 mM PMFS and 0.1% Triton X-100 were prepared using a Buckler gradient maker (Fort Lee, NJ, USA) and stored for 4 h at 4°C before use. The volume of each gradient was 12 ml. 500 μ L of 2% Triton X-100 extracts obtained from Torpedo electric organ (0.5-1 g labeled by incubation with 6 nM ^{125}I α Bgtx) and 500 μ L of a 2% Triton X-100 extract of either cortex and thalamus prepared from mice differing in $\alpha 4$ or $\beta 2$ genotype were loaded onto the gradients and centrifuged for 14 hours at 40,000 rpm in a Beckman SW41. Fractions of 0.5 ml were collected from the top of the gradient and directly counted on a γ counter (in the case of the Torpedo

Mol 45203

gradients), or added to the affinity-purified anti- $\alpha 4$ or anti- $\beta 2$ Abs bound to microwells and processed as previously described (Gotti et al 2005 a, b).

Affinity-purified anti- $\alpha 4$ or anti- $\beta 2$ Abs (10 $\mu\text{g/ml}$ in 50 mM phosphate buffer, pH 7.5) were bound to microwells (Maxi-Sorp, Nunc) by overnight incubation at 4°C. The following day, the wells were washed in order to remove excess unbound Abs. Then 100 μL aliquots of the gradient fractions that had been diluted 1: 2 with a buffer (TRIS-HCl, 50 mM, pH 7; NaCl, 150 mM ; KCl, 5 mM ; MgCl₂, 1 mM ; CaCl₂, 2.5 mM ;BSA, 2 mg/ml; and 0.05% Tween 20) were added to the wells and incubated overnight at 4°C. After this incubation, the wells were washed and immobilized receptors quantified using 1nM [³H]-epibatidine to label the binding sites. The wells were then washed seven times with ice-cold PBS containing 0.05% Tween 20, and the bound radioactivity was recovered by incubation with 200 μl of 2N NaOH for 2 hours. The bound radioactivity was then determined by beta counting.

The peak fractions of the gradients for samples of each of the different genotypes corresponding to the sedimentation coefficient of 10 S were pooled and concentrated by centrifugation in an Amicon Centricon filter (Millipore, Bedford, MA, USA) with a cutoff of 10,000 daltons, and the specific activity of these concentrated pools was determined

Immunoblotting

The protein obtained from concentrated gradient fractions was diluted 1:1(vol:vol) with Laemmli buffer and then underwent sodium dodecyl sulphate-polyacrylamide gel electrophoresis (SDS-PAGE) using 9% acrylamide.

For the experiments using constant protein levels, 5-10 μg of protein were loaded in each lane. For experiments using a constant number of binding sites, the amount of protein for each lane adjusted to have a constant number of binding sites per lane.

Mol 45203

After SDS-PAGE, the proteins were electrophoretically transferred to nitrocellulose membranes with 0.45 μ m pores (Schleicher and Schuell, Dassel, Germany). The blots were blocked overnight in 5% non-fat milk in Tris buffered saline (TBS), washed in a buffer containing 5% non fat-milk and 0.3% Tween 20 in TBS, incubated for 2 hours with the primary antibody (1–2.5 μ g/ml), and then incubated with the appropriate peroxidase conjugated secondary Abs. After another series of washes, peroxidase was detected using a chemiluminescent substrate (Pierce,Rockford,IL,USA)

Densitometric quantification of western blot bands

The signal intensity of the Western blot bands was acquired using an Epson 4500 gel scanner. The developed films were scanned as a Tiff scale in eight-bit grayscale format at setting of 300 dpi. All of the films obtained from the separate experiments of different $\alpha 4^{+/+}$, $\alpha 4^{+/-}$, and $\alpha 4^{-/-}$, $\beta 2^{+/+}$, $\beta 2^{+/-}$, and $\beta 2^{-/-}$ genotypes were acquired in the same way and scanned in parallel with the calibrated optical density step tablet from Stouffer (Mishawaka, IN, USA).

The images were analyzed using NIH Image J software (National Technical Information Service, Springfield, VA,USA). The pixel values of the images were transformed to optical density values by the program using the calibration curve obtained by acquiring the calibrated tablet with the same parameters as those used for the images.

The immunoreactive bands were quantified in 4–5 separate experiments for the cortex and three experiments for the thalamus. In the case of constant protein, the optical density ratio was calculated by taking the optical density of the WT as 1. The cortical values are the mean \pm SEM of four separate experiments for each genotype obtained from four separate sucrose gradient centrifugations; the thalamic values represent three separate experiments obtained from two different gradient centrifugations.

In the case of constant binding sites, the concentrated gradient fraction samples with the same number of [³H]-epibatidine binding sites were loaded in the lanes for wild-type ($\alpha 4^{+/+}$ and $\beta 2^{+/+}$) and for heterozygotic ($\alpha 4^{+/-}$ and $\beta 2^{+/-}$) preparations. In order to compare the signal intensity of the $\alpha 4$ and $\beta 2$ Ab labeling in wild-types and heterozygotes, the optical density ratio of relative expression was expressed as the heterozygote/wild-type ratio.

Data calculation and analyses.

Primary data from individual stimulations and ACh concentration-effect curves were analyzed using the non-linear least squares algorithm in Sigma Plot 2001 (Systat, San Jose, CA, USA). ACh-stimulated $^{86}\text{Rb}^+$ efflux was calculated as the increase in radioactivity above baseline and was normalized among samples and experiments by dividing by the basal efflux. Basal efflux was calculated by fitting the counts before and after the ACh-stimulated peak to a one-component exponential decay [$\text{EB}_t = \text{EB}_0 \cdot \exp(-k \cdot t)$, where EB_t is the amount of basal efflux at time, t ; EB_0 is the this value at $t=0$, and k is the first order decay constant]. ACh-stimulated efflux was calculated by subtracting basal efflux calculated from the exponential decay curve from the actual data and dividing by the basal efflux.

ACh concentration effect curves were fit to a two-component model: $E = E_{\text{hs}} \cdot \text{ACh} / (K_{\text{hs}} + \text{ACh}) + E_{\text{ls}} \cdot \text{ACh} / (K_{\text{ls}} + \text{ACh})$, where E is the total $^{86}\text{Rb}^+$ efflux at each concentration of ACh and E_{hs} and E_{ls} are the maximal $^{86}\text{Rb}^+$ efflux rates for the components with higher (K_{hs}) and lower (K_{ls}) sensitivity to stimulation by ACh. Initially, results for cortex and thalamus of mice of each genotype for which there were measurable responses ($\alpha 4^{+/+}$, $\alpha 4^{+/-}$, $\beta 2^{+/+}$ and $\beta 2^{+/-}$) were fit individually providing eight separate determinations of K_{hs} and K_{ls} . No significant differences in either K_{hs} (average value 2.5 μM) or K_{ls} (average value 140 μM) were observed between regions or among genotypes. Subsequently, results for each experiment were

Mol 45203

fit to the two component model with values for K_{hs} and K_{ls} fixed at 2.5 μ M and 140 μ M, respectively, to obtain estimates of V_{hs} and V_{ls} for every individual mouse.

SPSS (SPSS, Inc. Chicago, IL, USA) was used for the statistical analyses. Results were evaluated using Analysis of Variance (ANOVA). Initially, a two way ANOVA [nAChR subunit ($\alpha 4$ or $\beta 2$) and genotype (+/+, +/-, -/-)] was used to analyze the effect of deletion of each gene on both V_{hs} and V_{ls} in thalamus and cortex. Subsequently, the effect of each individual deletion was evaluated with one way ANOVA to compare activity in +/+, +/- and -/- for $\alpha 4$ and $\beta 2$ or by t-test to compare $\alpha 4$ and $\beta 2$ mice.

Mol 45203

Results.

nAChR Function in Cortical and Thalamic Synaptosomes of $\alpha 4$ and $\beta 2$ Mice

[125 I]-A85380 Binding in Synaptosomal Membranes.

[125 I]-A85380, which has been identified as a $\beta 2$ selective ligand (Mukhin et al., 2000), was used to measure binding sites in membrane preparations from mouse thalamic and cortical synaptosomes. In order to determine the effect of sequential deletion of the $\alpha 4$ or $\beta 2$ subunit on nicotinic binding sites in mouse cortex and thalamus, saturation curves for [125 I]-A85380 binding to membranes prepared from synaptosomes were constructed (Figure 1). Deletion of either the $\alpha 4$ or $\beta 2$ subunit had no significant effect on the apparent K_D for [125 I]-A85380 in either brain region, but the average apparent K_D value for cortex (3.7 pM) was slightly lower than that in thalamus (5.6 pM). No differences in [125 I]-A85380 binding were detected between the $\alpha 4^{+/+}$ and $\beta 2^{+/+}$ wild-type mice. A gene dose-dependent decrease in maximal [125 I]-A85380 binding was observed following deletion of either the $\alpha 4$ (cortex: $F_{2,9} = 247.9$, $p < 0.001$; thalamus: $F_{2,9} = 76.61$, $p < 0.001$) or the $\beta 2$ subunit (cortex: $F_{2,9} = 3737.9$, $p < 0.001$; thalamus: $F_{2,9} = 137.18$, $p < 0.001$). Binding was reduced by approximately one-half following deletion of a single copy of either gene in both brain regions ($\alpha 4$ thalamus $48.1 \pm 3.3\%$, $\beta 2$ thalamus $44.9 \pm 3.9\%$, $\alpha 4$ cortex $50.0 \pm 4.9\%$, $\beta 2$ cortex $44.6 \pm 0.9\%$) and by greater than 90% following deletion of either gene ($\alpha 4$ thalamus $93.7 \pm 0.9\%$, $\beta 2$ thalamus $97.6 \pm 2.1\%$, $\alpha 4$ cortex $96.1 \pm 2.1\%$ and $\beta 2$ cortex $98.5 \pm 2.5\%$). **Acetylcholine-Stimulated $^{86}\text{Rb}^+$ Efflux.**

Concentration effect curves for ACh-stimulated $^{86}\text{Rb}^+$ efflux from both cortical (Figure 2 A and D) and thalamic (Figure 3 A and D) synaptosomes of wild-type mice are biphasic. EC_{50} values for the higher and lower sensitivity components did not differ significantly between the

Mol 45203

brain regions and were unaffected by genotype (average EC_{50} for the higher sensitivity component = 2.5 μ M and for the lower sensitivity component = 140 μ M). The absolute and relative amounts of the $^{86}\text{Rb}^+$ efflux with higher and lower sensitivity to ACh stimulation differed between these regions and will be discussed in more detail below. Both phases of ACh-stimulated $^{86}\text{Rb}^+$ efflux were virtually eliminated by deletion of either the $\alpha 4$ or $\beta 2$ subunit in both regions.

Cortex.

The effect of partial or complete deletion of either the $\alpha 4$ or $\beta 2$ nAChR subunit on ACh-stimulated $^{86}\text{Rb}^+$ efflux in cortical synaptosomes is presented in Figure 2. The concentration-effect curves for the $\alpha 4$ and $\beta 2$ wild-type mice are both biphasic with approximately 70% of the response represented by the lower sensitivity component (Figures 2 A and D). No significant differences in ACh-stimulated release between the $\alpha 4^{+/+}$ and $\beta 2^{+/+}$ wild-type mice were noted for either the higher sensitivity ($\alpha 4 = 3.03 \pm 0.28$, $\beta 2 = 3.30 \pm 0.28$, $t_{26} = 0.86$, $p > 0.05$) or lower sensitivity ($\alpha 4 = 6.87 \pm 0.57$, $\beta 2 = 7.49 \pm 0.30$, $t_{26} = 0.53$, $p > 0.05$) components. Deletion of either subunit reduced ACh-stimulated $^{86}\text{Rb}^+$ efflux more than 90% such that the residual response in the null mutants was not significantly different from zero (Figures 2 C and F). Total ACh-stimulated $^{86}\text{Rb}^+$ efflux in either $\alpha 4^{+/-}$ (39% decrease) or $\beta 2^{+/-}$ (36% decrease) was significantly lower than that in wild-type mice and the extent of decrease observed for each heterozygote was similar. However, components of ACh-stimulated $^{86}\text{Rb}^+$ efflux with higher and lower ACh sensitivity were differentially affected by partial deletion of $\alpha 4$ and $\beta 2$ (Figure 2, panels G and H). A $26 \pm 9.6\%$ reduction in the higher sensitivity component was observed for $\alpha 4^{+/-}$ mice, while a $46 \pm 6.9\%$ reduction was observed for this component in $\beta 2^{+/-}$ mice (Figure 2G). A $49 \pm 6.9\%$ reduction in the lower sensitivity component was observed for $\alpha 4^{+/-}$ mice, while a $32 \pm 5.7\%$

Mol 45203

reduction was observed for $\beta 2^{+/-}$ mice. In addition, the residual lower sensitivity $^{86}\text{Rb}^+$ efflux in $\beta 2^{+/-}$ mice was significantly greater than that in $\alpha 4^{+/-}$ mice (4.93 ± 0.38 vs. 3.86 ± 0.44 , $t_{32}=2.14$, $p<0.05$). Thus, in cortical synaptosomes partial deletion of the $\alpha 4$ subunit ($\alpha 4^{+/-}$) produced a relatively larger decrease in the lower sensitivity component of ACh-stimulated $^{86}\text{Rb}^+$ efflux, while partial deletion of $\beta 2$ ($\beta 2^{+/-}$) produced a relatively larger decrease in the higher sensitivity component of ACh-stimulated $^{86}\text{Rb}^+$ efflux.

Thalamus.

The effect of partial deletion of either the $\alpha 4$ or $\beta 2$ nAChR subunit on ACh-stimulated $^{86}\text{Rb}^+$ efflux was also examined in thalamic synaptosomes and is presented in Figure 3. The concentration effect curves for $\alpha 4$ and $\beta 2$ wild-type mice were also biphasic. The higher sensitivity component comprised approximately 56% of total response in thalamic synaptosomes of wild-type mice (Figure 3 A and D). No significant differences between $\alpha 4^{+/+}$ and $\beta 2^{+/+}$ were noted for either the higher ($\alpha 4=14.14 \pm 0.39$, $\beta 2=15.87 \pm 0.42$, $t_{26}=1.01$, $p>0.05$) or lower ($\alpha 4=12.05 \pm 0.99$, $\beta 2=12.24 \pm 1.58$, $t_{26}=0.22$, $P>0.05$) sensitivity components.

Deletion of either subunit reduced both components by greater than 90% and the residual activity was not significantly different from zero (Figure 3 C and F). Similar to the results for cortex, total thalamic ACh-stimulated $^{86}\text{Rb}^+$ efflux was reduced approximately 40% following partial deletion of either the $\alpha 4$ ($\alpha 4^{+/-}$) or $\beta 2$ ($\beta 2^{+/-}$) subunit. Also similar to the results with cortex, when the ACh concentration effect curves were resolved into higher and lower sensitivity components differences between $\alpha 4^{+/-}$ and $\beta 2^{+/-}$ mice were observed (Figures 3 G and H). Partial deletion of the $\alpha 4$ subunit ($\alpha 4^{+/-}$) reduced the higher sensitivity $^{86}\text{Rb}^+$ efflux by $30 \pm 3.5\%$ and reduced lower sensitivity $^{86}\text{Rb}^+$ efflux by $51.0 \pm 6.9\%$. In contrast, partial deletion of $\beta 2$ subunit ($\beta 2^{+/-}$) reduced the higher sensitivity $^{86}\text{Rb}^+$ efflux by $54 \pm 2.4\%$ and reduced lower sensitivity

Mol 45203

$^{86}\text{Rb}^+$ efflux by $21 \pm 7.5\%$. Direct comparison of residual higher ($\alpha 4^{+/-} = 9.83 \pm 0.41$, $\beta 2^{+/-} = 7.23 \pm 0.33$, $t_{29} = 3.29$, $p < 0.05$) and lower ($\alpha 4^{+/-} = 5.96 \pm 0.75$, $\beta 2^{+/-} = 8.23 \pm 0.60$, $t_{29} = 2.17$, $p < 0.05$) sensitivity components revealed a differential effect of partial $\alpha 4$ and $\beta 2$ deletion in the respective heterozygotes. Thus, in thalamic synaptosomes partial deletion of the $\alpha 4$ subunit ($\alpha 4^{+/-}$) elicited a relatively larger decrease in the component of $^{86}\text{Rb}^+$ efflux with lower sensitivity to ACh, while partial deletion of the $\beta 2$ subunit ($\beta 2^{+/-}$) elicited a relatively larger decrease in the component with higher ACh sensitivity.

nAChR expression in the cortex and thalamus of mice differing in $\alpha 4$ and $\beta 2$ expression

The differential effects of partial $\alpha 4$ or $\beta 2$ nAChR subunit deletion on the higher and lower sensitivity components of ACh-stimulated $^{86}\text{Rb}^+$ efflux suggest that altering the relative expression of one of the subunits comprising the $\alpha 4\beta 2^*$ -nAChR subtype alters the functional properties of the receptor. In order to determine the effect of $\alpha 4$ and $\beta 2$ nAChR gene deletion on overall nAChR expression in the cortex and thalamus, ligand binding studies were performed using membranes prepared from wild-type ($\alpha 4^{+/+}$ or $\beta 2^{+/+}$), heterozygote ($\alpha 4^{+/-}$ or $\beta 2^{+/-}$) and null mutant ($\alpha 4^{-/-}$ or $\beta 2^{-/-}$) mice.

^3H -Epibatidine-binding nAChRs

^3H -Epibatidine binding was measured in membranes, extracts and concentrated gradient fractions obtained from each $\alpha 4$ and $\beta 2$ genotype (Table 1). The samples were incubated with 2 μM αBgtx for 3 hr before addition of [^3H]-epibatidine to block binding at αBtx -sensitive sites. Binding took place using a saturating concentration of [^3H]-epibatidine (2 nM).

Cortex

The density of cortical [^3H]-epibatidine binding nAChRs (in fmol/mg protein) was 64.9 ± 7.2 in $\alpha 4^{+/+}$ mice, 33.9 ± 3.3 in $\alpha 4^{+/-}$ mice and 2.5 ± 1.0 in $\alpha 4^{-/-}$ mice (mean \pm SEM of four

Mol 45203

experiments) and 76.4 ± 3.9 in $\beta 2^{+/+}$ mice, 41.4 ± 2.7 in $\beta 2^{+/-}$ mice and 2.0 ± 1.7 in $\beta 2^{-/-}$ (mean \pm SEM of four experiments). The effect of gene deletion measured for cortical tissue using [^3H]-epibatidine was comparable to that measured using [^{125}I]-A85380 in independent experiments (Figure 1). The specific activity of the 2% Triton X-100 was not different from that of the homogenate (Table 1). However, the specific activity of the concentrated gradient fraction samples from cortex was much higher than that of the 2% Triton X-100 extracts.

Thalamus

The density of thalamic [^3H]-epibatidine binding nAChRs (in fmol/mg protein) was 187.8 ± 23.8 in $\alpha 4^{+/+}$ mice, 105.0 ± 20.3 in $\alpha 4^{+/-}$ mice and 18.5 ± 9.2 in $\alpha 4^{-/-}$ mice (mean \pm SEM of four experiments) and 177.4 ± 10.6 in $\beta 2^{+/+}$ mice, 106.4 ± 15.2 in $\beta 2^{+/-}$ mice and 10.0 ± 3.4 in $\beta 2^{-/-}$ mice. The effect of gene deletion measured using [^3H]-epibatidine for thalamic tissue was comparable to that measured using [^{125}I]-A85380 (Figure 1). The specific activity of the extract was unchanged by 2% Triton x-100 extraction and the values are reported in Table 1. As in the case of cortex, the specific activity of concentrated gradient fractions prepared from thalamus was much higher than that of the 2% Triton X-100 extracts.

Subunit composition of cortical and thalamic [^3H]-epibatidine nAChRs

Cortex

The results described in the preceding paragraphs show that deletion of the $\alpha 4$ or $\beta 2$ subunit has measurable effects on overall nAChR expression, with an approximately 50% decrease in [^3H]-epibatidine binding sites in both $\alpha 4^{+/-}$ and $\beta 2^{+/-}$ mice. Samples were subsequently analyzed to determine whether gene deletion selectively affects the expression of some specific nAChR subtypes in heterozygotes and null mutants.

In order to quantify the relative contribution of each nicotinic subunit to [^3H]-epibatidine binding in the cortex, quantitative immunoprecipitation experiments were performed using subunit-specific antibodies and [^3H]-epibatidine labeled nAChRs on cortical tissue obtained from $\alpha 4^{+/+}$, $\alpha 4^{+/-}$, $\alpha 4^{-/-}$, $\beta 2^{+/+}$, $\beta 2^{+/-}$ and $\beta 2^{-/-}$ mice. Figure 4A shows the mean values of two separate experiments for each subunit in each genotype. The two major subtypes in both $\alpha 4^{+/+}$ and $\beta 2^{+/+}$ cortex were the $\alpha 4\beta 2$ (80-85% of all [^3H]-epibatidine binding sites) and the $\alpha 4\alpha 5\beta 2$ (10-15%). In heterozygotes the total number of $\alpha 5$ -containing subtypes (expressed as fmol/mg of protein) was significantly reduced (from 8.3 in $\alpha 4^{+/+}$ to 4.8 in $\alpha 4^{+/-}$ and from 8.4 in $\beta 2^{+/+}$ to 4.8 in $\beta 2^{+/-}$) but the percentage of [^3H]-epibatidine-labeled $\alpha 5$ -containing receptors was the same in wild-type and heterozygotes (16-18%). The cortex also contained small amounts of $\alpha 6^*$ -nAChR and $\alpha 3^*$ -nAChR, but the levels of these minor receptors were unchanged in the heterozygotes and remained at the limit of our immunoprecipitation detection. The heterozygotes showed a selective decrease in the number of total [^3H]-epibatidine binding sites, because of the decrease in the $\alpha 4\beta 2$ -nAChR and $\alpha 4\alpha 5\beta 2$ -nAChR. However, the ratio of these two subtypes did not differ between heterozygotes and wild-types.

Thalamus

The [^3H]-epibatidine-binding nAChRs expressed in thalamus of wild-type mice are slightly more heterogeneous than those expressed in the cortex. [^3H]-Epibatidine binding sites containing solely $\alpha 4$ and $\beta 2$ subunits represent 70-80% of the total in $\alpha 4$ and $\beta 2$ wild-types, and an additional 10% of the $\alpha 4\beta 2^*$ -nAChR also include the $\alpha 5$ subunit. In addition, [^3H]-epibatidine binding sites containing $\alpha 3$ and $\beta 4$ subunits comprise 6-7% in the sites in $\alpha 4^{+/+}$ and 8-10 % of the sites in the $\beta 2^{+/+}$ thalamus (Figure 4B). Approximately 5-6 % of the [^3H]-

epibatidine binding nAChRs contained the $\alpha 5$ subunit and 8-10% the $\beta 3$ subunit in wild-type mice of both genotypes.

A decrease in $\alpha 4$, $\alpha 5$ and $\beta 2$ subunit expression of approximately 50% from that in wild-types was observed in both $\alpha 4^{+/-}$ and $\beta 2^{+/-}$ thalamus, whereas the levels of the $\alpha 3$ and $\beta 4$ subunits were unchanged, and those of the $\beta 3$ were only slightly decreased. In order to determine whether $\alpha 3$, $\beta 4$ and $\beta 3$ subunits can be present in subtypes other than the $\alpha 4\beta 2$ -nAChR, parallel immunoprecipitation experiments were performed using $\alpha 4^{-/-}$ and $\beta 2^{-/-}$ mice. As shown in Figure 4B, the only subtype present in the thalamus of the null mutant mice was $\alpha 3\beta 4\beta 3$ -nAChR, which was present at a level similar to that of wild-type.

In conclusion, these immunoprecipitation data indicate that the large majority of receptors in the thalamus (70-80%) are $\alpha 4\beta 2$ -nAChR, 10% $\alpha 4\alpha 5\beta 2$ -nAChR and approximately 10% $\alpha 3\beta 3\beta 4$ -nAChR.

Sucrose gradient analysis of nAChRs in the cortex and thalamus of $\alpha 4$ and $\beta 2$ mice

In order to ascertain whether the $\alpha 4$ and $\beta 2$ subunits were incorporated into correctly-assembled pentameric subtypes in mice, the nAChRs were fractionated using sucrose density-gradient centrifugation, and only the detergent-solubilized nAChRs of the correct size were analyzed by Western blots. Figure 5 shows the gradient profiles of cortical extracts prepared from $\alpha 4^{+/+}$, $\alpha 4^{+/-}$, $\beta 2^{+/+}$ and $\beta 2^{+/-}$ mice. Following centrifugation, nAChRs within each fraction were captured using anti- $\alpha 4$ and anti- $\beta 2$ Ab-coated wells, and then quantitated by [3 H]-epibatidine binding. The detergent solubilized nAChRs sedimented as a single species that was slightly larger than Torpedo AChR monomers. These results clearly indicate that, although reduced in number, both the $\alpha 4^{+/-}$ and $\beta 2^{+/-}$ have a correct pentameric assembly. Moreover,

Mol 45203

these sedimentation experiments confirmed that the level of expression of assembled $\alpha 4\beta 2$ nAChR was lower in heterozygotes, consistent with the immunoprecipitation results described above (Figure 4A).

Qualitatively similar results were obtained on thalamic nAChRs separated on sucrose gradient (data not shown).

Western blot analysis of $\alpha 4$ and $\beta 2$ subunit expression

As shown above and as previously reported, the major subtypes expressed in the cortex and thalamus are the $\alpha 4\beta 2$ -nAChR and $\alpha 4\alpha 5\beta 2$ -nAChR subtypes. The immunoprecipitation studies clearly showed that the 50% reduction in [^3H]-epibatidine binding sites in the $\alpha 4^{+/-}$ and $\beta 2^{+/-}$ genotypes is due to the loss of $\alpha 4\beta 2$ -nAChR and $\alpha 4\alpha 5\beta 2$ -nAChR subtypes.

The specificity of our Abs were tested by incubating blots obtained from the cortex of wild-type and null mutant $\alpha 4$ and $\beta 2$ mice with Abs directed against the $\alpha 4$ or $\beta 2$ subunits after the electrophoresis of 10 μg of 2 % Triton extract. As shown in Figure 6, the anti- $\alpha 4$ Ab recognized a peptide with a molecular mass of approximately 68-72kDa (corresponding to the expected size of the $\alpha 4$ subunit), in the extract taken from the wild-type but not $\alpha 4^{-/-}$ mice (Figure 6A left) and the anti- $\beta 2$ Ab recognized a band of 52 kDa (corresponding to the expected size of the $\beta 2$ subunit), in the extract taken from the wild-type but not $\beta 2^{-/-}$ mice (Figure 6A right).

The immunoprecipitation studies (Figure 4) indicated that 8-10% of the thalamic [^3H]-epibatidine binding nAChRs in both wild-types contain the $\alpha 3$ and $\beta 4$ subunits. In order to exclude a possible antibody cross-reactivity, the $\alpha 4\beta 2$ subtype from $\beta 2^{+/-}$ cortex was

Mol 45203

immunopurified over an affinity column with bound anti- $\beta 2$ Abs and probed with the anti $\alpha 4$, $\beta 2$, $\alpha 5$, $\alpha 3$, $\beta 3$ and $\beta 4$ Abs. As shown in Figure 6B, the purified $\alpha 4\beta 2^*$ -nAChR subtype was labeled by the anti- $\alpha 4$, anti- $\alpha 5$, and anti- $\beta 2$ Abs but not by the anti- $\alpha 3$, $\beta 3$, $\beta 4$ Abs thus further indicating that the Abs raised to $\alpha 4$ and $\beta 2$ subunits detect only the target subunit.

Cortex

Samples obtained from $\alpha 4^{+/+}$, $\alpha 4^{+/-}$, $\alpha 4^{-/-}$ $\beta 2^{+/+}$, $\beta 2^{+/-}$ and $\beta 2^{-/-}$ mice were analyzed by loading the same amount of protein of fully assembled receptors obtained after sucrose gradient centrifugation.

Figure 7A shows typical anti- $\alpha 4$ and anti- $\beta 2$ Ab labeling of samples obtained by loading the same amount of protein after sucrose gradient centrifugation. Figure 7B shows the signal intensity for the $\alpha 4$ and $\beta 2$ subunits in the different genotypes expressed as the ratio of Ab labeling (taking the amount present in the samples from wild-type mice as 1) as shown by the results of four independent experiments using four separate sucrose gradients. The mean \pm SEM optical density ratios of the $\alpha 4$ subunit in the $\alpha 4$ genotype were 1.0 ± 0.0 in the $\alpha 4^{+/+}$, 0.41 ± 0.02 in the $\alpha 4^{+/-}$ and 0.04 ± 0.02 in the $\alpha 4^{-/-}$, and those of the $\beta 2$ subunit were 1.0 ± 0.0 in the $\alpha 4^{+/+}$, 0.50 ± 0.02 in the $\alpha 4^{+/-}$ and 0.01 ± 0.006 in the $\alpha 4^{-/-}$ genotypes.

A Mann-Whitney test indicated significant differences in the normalized optical densities of the $\alpha 4^{+/+}$, $\alpha 4^{+/-}$ and $\alpha 4^{-/-}$ ($P < 0.001$), and that the $\alpha 4$ (0.41) and $\beta 2$ (0.50) subunit ratios in $\alpha 4^{+/-}$ were also significantly different (* $P = 0.038$).

Among the mice with different $\beta 2$ expressions, the mean \pm SEM optical density ratios of the $\alpha 4$ subunit were 1.0 ± 0.0 in the $\beta 2^{+/+}$, 0.49 ± 0.01 in the $\beta 2^{+/-}$ and 0.12 ± 0.02 in the $\beta 2^{-/-}$ genotypes, and those of the $\beta 2$ subunit were respectively 1.0 ± 0.0 , 0.32 ± 0.006 and 0.02 ± 0.001 .

Mol 45203

A Mann-Whitney test showed significant difference in the normalized optical densities of the $\beta 2^{+/+}$, $\beta 2^{+/-}$ and $\beta 2^{-/-}$ ($P < 0.001$), and that the $\alpha 4$ (0.49) and $\beta 2$ (0.32) subunit ratios in $\beta 2^{+/-}$ were also significantly different ($***P = 0.0004$).

Immunoblotting experiments performed using constant protein for each of the six genotypes suggested that the ratio of the $\alpha 4$ and $\beta 2$ subunits was different in the preparations from the $\alpha 4^{+/+}$, $\beta 2^{+/+}$, $\alpha 4^{+/-}$ and $\beta 2^{+/-}$ mice, and so the $\alpha 4$ and $\beta 2$ subunits in the assembled receptors were measured using a different quantitative approach. The same number of binding sites of the sucrose gradient centrifugation fractions of the wild-types (lanes 1 and 2) and the heterozygotes (lanes 3 and 4) were loaded onto the same gel, after which the blots were probed with anti- $\alpha 4$ Ab and then stripped and probed with anti- $\beta 2$ Ab (or vice-versa). Figure 8A (left) shows the labeling of the same number of binding sites by the anti- $\alpha 4$ (upper part) and the anti- $\beta 2$ Ab (lower part) in the $\alpha 4^{+/+}$ (lanes 1 and 2) and $\alpha 4^{+/-}$ genotypes (lanes 3 and 4) and Figure 8A (right) shows the labeling of the same number of binding sites by the anti- $\alpha 4$ (upper part) and anti- $\beta 2$ Ab (lower part) in the $\beta 2^{+/+}$ (lanes 1 and 2) and $\beta 2^{+/-}$ genotypes (lanes 3 and 4). Four separate sucrose gradient fraction samples for each genotype were measured using 1 fmol or 2 fmol of binding sites per lane. The results, shown in Figure 8B are expressed as the ratio between the optical density of the heterozygotes divided by the optical density of the wild-types. The heterozygote/ wild-type ratios for $\alpha 4^{+/-}/\alpha 4^{+/+}$ were 0.85 ± 0.05 for the $\alpha 4$ subunit Ab and 1.2 ± 0.05 for the $\beta 2$ subunit Ab (Mann-Whitney test, $**P = 0.0022$) whereas the ratios in the $\beta 2^{+/-}/\beta 2^{+/+}$ were 1.4 ± 0.1 and 0.78 ± 0.08 (Mann-Whitney test, $**P = 0.0022$).

These data do not allow the assignment of the exact stoichiometry and ratios of the $\alpha 4\beta 2$ -nAChR in wild-type and heterozygote cortex because the immunological signals of the

Mol 45203

$\alpha 4$ and $\beta 2$ subunits depend on the reactivity of the anti- $\alpha 4$ and anti- $\beta 2$ Abs, which may be different. However, the $\alpha 4/\beta 2$ ratios for the same number of binding sites were different for the $\alpha 4^{+/-}$ and the $\beta 2^{+/-}$ cortices, thus strongly suggesting that there is a difference in $\alpha 4$ and $\beta 2$ subunit content between $\alpha 4^{+/-}$ and $\beta 2^{+/-}$ mice. The fact that the heterozygote/ wild-type ratios for the $\alpha 4$ and $\beta 2$ subunits were respectively 0.85 ± 0.05 and 1.2 ± 0.05 in the $\alpha 4$ genotype indicates that there are more receptors with the possible $(\alpha 4)_2(\beta 2)_3$ stoichiometry in $\alpha 4^{+/-}$ than in $\alpha 4^{+/+}$, and the fact that the ratios for the $\alpha 4$ and $\beta 2$ subunits were respectively 1.4 ± 0.1 and 0.78 ± 0.08 indicates that a higher content of receptors with the $(\alpha 4)_3(\beta 2)_2$ subunit stoichiometry in the $\beta 2^{+/-}$ than in the $\beta 2^{+/+}$.

Thalamus

Sucrose gradient fractions prepared from thalamic tissue were also analyzed by quantitative Western blotting. The results of three independent experiments using two separate sucrose gradients are shown in Figure 9.

In the mice with different $\alpha 4$ expression, the mean \pm SEM optical density ratios for the $\alpha 4$ subunit were 1.0 ± 0.0 in $\alpha 4^{+/+}$, 0.46 ± 0.03 in $\alpha 4^{+/-}$ and 0.04 ± 0.01 in $\alpha 4^{-/-}$, and those of the $\beta 2$ subunit were 1.0 ± 0.0 in $\alpha 4^{+/+}$, 0.54 ± 0.04 in $\alpha 4^{+/-}$ and 0.03 ± 0.002 in the $\alpha 4^{-/-}$. A Mann-Whitney test showed significant difference in the normalized optical densities of $\alpha 4^{+/+}$, $\alpha 4^{+/-}$ and $\alpha 4^{-/-}$ mice ($P < 0.01$), and the $\alpha 4$ (0.46) and $\beta 2$ (0.54) subunit ratios ($\alpha 4^{+/-}/\alpha 4^{+/+}$) were not significantly different from each other.

In the mice with different $\beta 2$ expression, the mean \pm SEM optical density ratios for the $\alpha 4$ subunit were 1.0 ± 0.0 in $\beta 2^{+/+}$, 0.56 ± 0.07 in $\beta 2^{+/-}$ and 0.12 ± 0.04 in $\beta 2^{-/-}$, and those of the $\beta 2$ subunit were 1.0 ± 0.0 , 0.33 ± 0.002 and 0.02 ± 0.002 , respectively. A Mann-Whitney test

Mol 45203

showed significant differences in the normalized optical densities of both the $\alpha 4$ and $\beta 2$ subunits in the $\beta 2^{+/+}$, $\beta 2^{+/-}$ and $\beta 2^{-/-}$ mice ($P < 0.001$). The relative expression of the $\alpha 4$ (0.56) and $\beta 2$ (0.33) subunits in heterozygotes relative to wild-type were differentially affected by partial deletion of the $\beta 2$ gene ($\beta 2^{+/-}$) and differed significantly from each other ($*P = 0.015$).

Additional blot experiments were performed on thalamus in which the same number of binding sites from sucrose gradient fractions was loaded onto the same gel for direct comparison of the ratio of $\alpha 4$ and $\beta 2$ subunits in the wild-types and heterozygotes. The blots were probed with anti- $\alpha 4$ Ab, and then stripped and probed with anti- $\beta 2$ Abs (or vice versa). Figure 10A (left) shows the labeling of the same number of binding sites by anti- $\alpha 4$ (upper part) and anti- $\beta 2$ Ab (lower part) in the $\alpha 4^{+/+}$ (lanes 1 and 2) and $\alpha 4^{+/-}$ genotypes (lanes 3 and 4), and Figure 10A (right) the labeling of the same number of binding sites by the anti- $\alpha 4$ (upper part) and anti- $\beta 2$ Ab (lower part) in $\beta 2^{+/+}$ (lanes 1 and 2) and $\beta 2^{+/-}$ genotypes (lanes 3 and 4). Three separate sucrose gradient fraction samples were tested for each genotype.

The results, shown in Figure 10B are expressed as the ratio between the optical density of the heterozygote and wild-type genotype measured using 1 fmol or 2 fmol of binding sites per lane. The mean optical density ratios \pm SEM for the $\alpha 4^{+/-}/\alpha 4^{+/+}$ ratios were 0.80 ± 0.05 for the $\alpha 4$ subunit and 1.53 ± 0.09 for the $\beta 2$ subunit (Mann-Whitney test, $*P = 0.029$), and those for the $\beta 2^{+/-}/\beta 2^{+/+}$ genotype were 1.44 ± 0.09 for the $\alpha 4$ subunit and 0.9 ± 0.1 for the $\beta 2$ subunit (Mann-Whitney test, $**P = 0.0079$).

Discussion

As previously reported (Marks et al., 1999; Butt et al., 2003; Brown et al., 2007) and confirmed here (Figures 2 and 3) ACh-stimulated $^{86}\text{Rb}^+$ efflux from cortical and thalamic synaptosomes is biphasic with components displaying high ($\text{EC}_{50} \approx 2 \mu\text{M}$) and low ($\text{EC}_{50} \approx 100 \mu\text{M}$) sensitivity to activation by ACh. Both components in these regions are primarily $\alpha 4\beta 2^*$ -nAChR since deletion of either $\alpha 4$ (Marks et al., 2007) or $\beta 2$ (Marks et al., 1999, 2000) subunit virtually eliminated them. $\alpha 4\beta 2$ -nAChRs expressed in *Xenopus laevis* oocytes or embryonic kidney cells also display biphasic ACh concentration effect curves with EC_{50} values comparable to those measured for $^{86}\text{Rb}^+$ efflux (Zwart and Vijverberg, 1998; Nelson et al., 2003; Khiroug et al., 2004; Moroni et al., 2006). The relative expression of the two components can be modified by injecting differing ratios of the mRNAs for the $\alpha 4$ and $\beta 2$ subunits. Oocytes injected with a large excess of $\beta 2$ mRNA express primarily the high sensitivity responses, while oocytes injected with a large excess of $\alpha 4$ mRNA express primarily the low sensitivity responses (Zwart and Vijverberg, 1998; Nelson et al., 2003; Moroni et al., 2006), leading to the postulate that differential sensitivity to agonist stimulation results from differences in $\alpha 4\beta 2$ -nAChR subunit stoichiometry [$(\alpha 4)_2(\beta 2)_3$ for high and $(\alpha 4)_3(\beta 2)_2$ for low]. Compelling evidence that supports the assertion that subunit stoichiometry influences sensitivity to agonists was obtained in studies with linked $\alpha 4/\beta 2$ subunits that were expressed with either an additional $\beta 2$ or $\alpha 4$ subunit (Zhou et al., 2003; Tapia et al., 2007). These manipulations resulted in expression of either high or low sensitivity receptors, respectively

Since alteration of relative $\alpha 4$ and $\beta 2$ expression changes receptor stoichiometry in heterologous expression systems, heterozygous $\alpha 4^{+/-}$ and $\beta 2^{+/-}$ mice were used in current study to evaluate the effects of manipulation of mouse brain mRNA levels *in vivo* on protein expression and receptor function. Previously, we reported that deletion or partial deletion of either $\alpha 4$ or $\beta 2$ reduced mRNA levels for the target subunit without affecting mRNA levels of the complementary subunit (Whiteaker et al., 2006). Here we report that partial deletion of either the $\alpha 4$ ($\alpha 4^{+/-}$) or $\beta 2$ ($\beta 2^{+/-}$) subunit gene decreased the expression of $\alpha 4\beta 2^*$ -nAChRs measured by [^{125}I]-A85380 binding to synaptosomal membranes (Figure 1) and [^3H]-

epibatidine binding precipitated by both the anti- $\alpha 4$ and the anti- $\beta 2$ antibodies (Table 1, Figure 4) in both the cortex and thalamus by 50%. Furthermore, this decrease in binding reflects a decrease in the number of properly assembled receptors determined by sucrose gradient centrifugation (Figure 5).

In the current study, we observed that both components of ACh-stimulated $^{86}\text{Rb}^+$ efflux were reduced in $\alpha 4^{+/-}$ and $\beta 2^{+/-}$ cortex and thalamus. If the stoichiometry of the $\alpha 4\beta 2^*$ -nAChR was unaffected by partial deletion of either the $\alpha 4$ or $\beta 2$ subunit, the proportion of these two components should remain unchanged in tissue obtained from the heterozygous mice. However, partial deletion of the $\alpha 4$ subunit (this should favor the formation of $(\alpha 4)_2(\beta 2)_3$ nAChRs) resulted in a relatively larger decrease in the lower sensitivity component, whereas partial deletion of the $\beta 2$ subunit (this should favor the formation of $(\alpha 4)_3(\beta 2)_2$ nAChRs) resulted in a relatively larger decrease in the higher sensitivity component. These results are consistent with the hypothesis that the stoichiometry of $\alpha 4\beta 2^*$ -nAChR is affected by the relative expression of $\alpha 4$ and $\beta 2$ mRNA *in vivo* and are in agreement with the results observed in heterologous expression systems.

In order to test whether subunit expression was actually changed by partial gene deletion, Western blots with subunit specific Abs were used to analyze the subunit content of correctly assembled pentameric receptors fractionated on sucrose gradients. No signal was obtained using extracts from $\alpha 4^{-/-}$ or $\beta 2^{-/-}$ mice thereby demonstrating that the Abs used in this study were specific. Such analysis is essential since specificity of different batches of polyclonal Abs prepared in different rabbits can vary between techniques and even when using the same technique (Gotti et al., 2006). The extent of the deletion on [^3H]-epibatidine binding was greater for the $\beta 2$ subunit, which was completely absent from the cortex and thalamus of $\alpha 4^{-/-}$ mice, while a residual 10 % of $\alpha 4$ immunoreactivity was still present in $\beta 2^{-/-}$ mice. These results are generally consistent with our histochemical analyses of these same gene deletions using different antibodies (Whiteaker et al, 2006).

Since, except for the target $\alpha 4$ and $\beta 2$ genes and also the $\alpha 5$ gene, partial or complete deletion of either the $\alpha 4$ or $\beta 2$ subunit did not alter the expression profile for other cortical or thalamic nAChR

proteins (Figure 4). If stoichiometry were unchanged by partial gene deletion, the ratios of $\alpha 4:\beta 2$ in the $\alpha 4^{+/-}$ and $\beta 2^{+/-}$ would be expected to be the same as those seen in the wild type control mice. One definitive way of determining receptor stoichiometry is to measure the number of $\alpha 4$ and $\beta 2$ subunits in fully assembled receptors by metabolically labeling the proteins as has been done in the case of chick and rat $\alpha 4\beta 2$ subtypes expressed in heterologous systems (Anand et al 1991; Nelson et al 2003). However, this is not feasible *in vivo*. As an alternative approach assembled receptors were quantitated immunologically. Labeling native receptors with anti- $\alpha 4$ and anti- $\beta 2$ Abs cannot define the stoichiometry of WT receptors because the immunolabeling depends on the avidity of the Abs and because the relationship between the amount of subunit and signal intensity is linear only in a narrow window. Considering these limitations, careful quantitation of Ab labeling intensity using the same amount of protein or the same number of binding sites from wild type and heterozygous mice, yielded data that suggest that the ratio of $\alpha 4$ and $\beta 2$ subunit protein in assembled $\alpha 4\beta 2$ nAChRs differ between control and heterozygous mutant mice. In both cortex and thalamus relative expression of the $\alpha 4$ subunit is lower than that of the $\beta 2$ subunit in $\alpha 4^{+/-}$ genotype whereas relative expression of the $\alpha 4$ subunit is higher than that of the $\beta 2$ in $\beta 2^{+/-}$ mice. These results are consistent with an altered stoichiometry of $\alpha 4\beta 2^*$ -nAChR following partial gene deletion such that $\alpha 4^{+/-}$ have more receptors with a stoichiometry of $(\alpha 4)_2(\beta 2)_3$ and $\beta 2^{+/-}$ have more receptors with a stoichiometry of $(\alpha 4)_3(\beta 2)_2$.

The consequences of partial $\alpha 4$ or $\beta 2$ deletion determined with the immunochemical studies parallel those of partial gene deletion on $^{86}\text{Rb}^+$ efflux. The relatively larger decrease in the lower sensitivity component of ACh –stimulated $^{86}\text{Rb}^+$ efflux in $\alpha 4^{+/-}$ and a relatively larger decrease in the higher sensitivity component in the $\beta 2^{+/-}$ is consistent with the changes in relative subunit expression in the heterozygous mice determined by Ab labeling.

An important consideration associated with studying brain is that many different nAChRs might be present. We chose cortex and thalamus for the studies reported here because gene deletion experiments

Mol 45203

showed that almost all [^3H]-epibatidine binding sites (Marks et al., 2006; 2007) and $^{86}\text{Rb}^+$ efflux (Marks et al., 2000, 2007) in these brain regions are $\alpha 4\beta 2$ with a small fraction of $\alpha 4\alpha 5\beta 2$ (Brown et al., 2007). The immunological studies (Figure 4) support this postulate. Most of the signal in cortex is clearly $\alpha 4\beta 2$; $\alpha 5$ subunits that coassemble with $\alpha 4$ and $\beta 2$ represent 10-15% of the total $\alpha 4\beta 2^*$ -nAChR binding sites in thalamus (Figure 4 and Gotti et al 2006). These $\alpha 4\beta 2\alpha 5$ -nAChRs seem to mediate more than 10-15% of total ACh-stimulated ion flux in thalamus, but very little of this response in cortex (Brown et al., 2007).

The evidence presented here strongly suggests that $\alpha 4\beta 2$ -nAChR differing in subunit stoichiometry exist *in vivo*. The higher and lower sensitivity components show different pharmacological profiles for both agonists and antagonists in brain (Marks et al., 1999) and in heterologous expression systems (Moroni et al. 2006). The two components also differ in calcium permeability (Tapia et al., 2007) and in up-regulation following chronic nicotine exposure both *in vitro* (Buisson and Bertrand, 2001; Nelson et al 2003; Kuryatov et al 2005) and treatment *in vivo* (Marks et al., 2004). The relative expression of the two components also differs across mouse brain regions (Marks et al., 2000, 2007) suggesting that relative effects of nicotinic drugs could vary among brain regions. Furthermore, using heterologous expression systems differences in the either untranslated regions of the gene (Briggs et al., 2006) or naturally occurring polymorphisms in the coding regions (Kim et al., 2003) affect relative expression $\alpha 4\beta 2$ -nAChR with higher or lower ACh sensitivity. The demonstration that natively expressed $\alpha 4\beta 2$ -nAChR very likely have alternative stoichiometries, which can be influenced by the relative level of expression of mRNA encoding the $\alpha 4$ and $\beta 2$ subunits, supports the results obtained using heterologous expression systems and implies that these alternatively assembled receptors could have important consequences *in vivo*.

References.

- Anand R, Conroy WG, Schoepfer R, Whiting P and Lindstrom J (1991) Neuronal nicotinic acetylcholine receptors expressed in *Xenopus* oocytes have a pentameric quaternary structure. *J Biol Chem* **266**:11192-11198.
- Badio B, Daly JW (1994) Epibatidine, a potent analgetic and nicotinic agonist. *Mol Pharmacol* **45**:563-569.
- Briggs CA, Gubbins EJ, Marks MJ, Putman CB, Thimmapaya R, Meyer MD and Surowy CS (2006) Untranslated region-dependent exclusive expression of high-sensitivity subforms of $\alpha 4\beta 2$ and $\alpha 3\beta 2$ nicotinic acetylcholine receptors. *Mol Pharmacol* **70**:227-240.
- Buisson B and Bertrand D (2001) Chronic exposure to nicotine upregulates the human $\alpha 4\beta 2$ nicotinic acetylcholine receptor function. *J Neurosci* **21**:1819-1829.
- Champtiaux N, Gotti C, Cordero-Erausquin M, David DJ, Przybylski C, Lena C, Clementi F, Moretti M, Rossi FM, LeNovere N, McIntosh JM, Gardier AM and Changeux J-P (2003) Subunit composition of functional nicotinic receptors in dopaminergic neurons investigated with knock-out mice. *J Neurosci* **23**:7820-7829.
- Cooper E, Couturier S and Ballivet M (1991) Pentameric structure and subunit stoichiometry of a neuronal nicotinic acetylcholine receptor. *Nature* **350**:235-238.
- Covert POJ and Connolly JG (2000) Multiple components in the agonist concentration-response relationships of neuronal nicotinic acetylcholine receptors. *J Neurosci Meth* **96**:63-70.
- Davila-Garcia MI, Musachio LJ, Perry DC., Xiao Y, Horti A, London ED, Dannals RF and Kellar KJ (1997) [125I]IPH, an epibatidine analog, binds with high affinity to neuronal nicotinic cholinergic receptors. *J Pharmacol Exp Ther* **282**:445-451.

Mol 45203

- Flores CM, Rogers SW, Pabreza LA, Wolfe BB, Kellar KJ (1992) A subtype of nicotinic cholinergic receptor in rat brain is composed of $\alpha 4$ and $\beta 2$ subunits and is up-regulated by chronic nicotine treatment. *Mol Pharmacol*. **41**:31-37.
- Gotti C, Moretti M, Clementi F, Riganti L, McIntosh JM, Collins AC, Marks MJ and Whiteaker P (2005a) Expression of nigrostriatal $\alpha 6$ -containing nicotine acetylcholine receptors is selectively reduced, but not eliminated, by $\beta 3$ subunit gene deletion. *Mol Pharmacol* **67**:2007-2015.
- Gotti C, Moretti M, Zanardi A, Gaimarri A, Champiaux N, Changeux JP, Whiteaker P, Marks MJ, Clementi F, Zoli M (2005b) Heterogeneity and selective targeting of neuronal nicotinic acetylcholine receptor (nAChR) subtypes expressed on retinal afferents of the superior colliculus and lateral geniculate nucleus: identification of a new native nAChR subtype $\alpha 3\beta 2(\alpha 5$ or $\beta 3)$ enriched in retinocollicular afferents. *Mol Pharmacol* **68**:1162-1171.
- Gotti C, Zoli M and Clementi F (2006) Brain nicotinic acetylcholine receptors: native subtypes and their relevance. *Trends Pharmacol Sci* **27**(9):482-491.
- Houghtling RA, Davila-Garcia MI, Kellar KJ (1995) Characterization of (+/-)-[³H]epibatidine binding to nicotinic cholinergic receptors in rat and human brain. *Mol Pharmacol* **48**: 280-287.
- Khiroug SS, Khiroug L and Yakel JL (2004) Rat nicotinic acetylcholine receptor $\alpha 2\beta 2$ channels: Comparison of functional properties with $\alpha 4\beta 2$ channels in *Xenopus* oocytes. *Neuroscience* **124**:817-822.
- Kim H, Flanagan BA, Qin C, Macdonald RL, Stitzel JA (2003) The mouse ChRNA4 A529T polymorphism alters the ratio of high and low affinity $\alpha 4\beta 2$ nAChRs, *Neuropharmacology* **45**:345-354.
- Lindstrom J (2000) The structure of nAChRs, in Neuronal Nicotinic Receptors, Handbook of Experimental Pharmacology, Vol 144 (Clementi F, Fornasari D and Gotti C eds) pp 101-162 Springer-Verlag, Berlin.

Mol 45203

Lowry OH, Rosebrough NJ, Farr AL and Randall RJ (1951) Protein measurement with the Folin phenol reagent. *J Biol Chem* **193**:265-275.

Marks MJ, Smith KW, Collins AC (1998) Differential agonist inhibition identifies multiple epibatidine binding sites in mouse brain. *J Pharmacol Exp Ther* 285:377-386.

Marks MJ, Whiteaker P, Calcaterra J, Stitzel JA, Bullock AE, Grady SR, Picciotto MR, Changeux J-P, Collins AC (1999) Two pharmacologically distinct components of nicotinic receptor-mediated rubidium efflux in mouse brain require the $\beta 2$ subunit. *J Pharmacol Exp Ther* 289:1090-1103.

Marks MJ, Stitzel JA, Grady SR, Picciotto MR, Changeux J-P and Collins AC (2000) Nicotinic-agonist stimulated $^{86}\text{Rb}^+$ efflux and [^3H]epibatidine binding of mice differing in $\beta 2$ genotype. *Neuropharmacology* **39**:2532-2645.

Marks MJ, Rowell PP, Cao J-Z, Grady SR, McCallum SE and Collins AC (2004) Subsets of acetylcholine-stimulated $^{86}\text{Rb}^+$ efflux and [^{125}I]-epibatidine binding sites in C57BL/6 mouse brain are differentially affected by chronic nicotine treatment. *Neuropharmacology* **46**:1141-1157.

Marks MJ, Whiteaker P and Collins AC (2006) Deletion of the $\alpha 7$, $\beta 2$ or $\beta 4$ nicotinic receptor subunit genes identifies highly expressed subtypes with relatively low affinity for [^3H]epibatidine. *Mol Pharmacol* **70**:947-959.

Marks MJ, Meinerz NM, Drago J and Collins AC (2007) Gene targeting demonstrates that $\alpha 4$ nicotinic acetylcholine receptor subunits contribute to the expression of diverse [^3H]epibatidine binding sites and components of biphasic $^{86}\text{Rb}^+$ efflux with high and low sensitivity to stimulation by acetylcholine. *Neuropharmacology* **53**:390-405.

Marubio LM, Arroyo-Jimenex MD, Cordero-Erausquin M, Lena C, LeNovere N, d'Exaerde AD, Huchet M, Damaj MI and Changeux J-P (1999) Reduced antinociception in mice lacking neuronal nicotinic receptor subunits. *Nature* **398**:805-810.

Mol 45203

Moretti M, Vailati S, Zoli M, Lippi G, Riganti L, Longhi R, Viegi A, Clementi F, Gotti C. (2004)

Nicotinic acetylcholine receptor subtypes expression during rat retina development and their regulation by visual experience. *Mol Pharmacol* **66**:85-96.

Moroni M, Zwart R, Sher E, Cassels BK and Bermudez I (2006) $\alpha 4\beta 2$ nicotinic receptors with high and low acetylcholine sensitivity: pharmacology, stoichiometry, and sensitivity to long-term exposure to nicotine. *Mol Pharmacol* **70**(2):755-768.

Mukhin AG, Gundish D, Horti AG, Koren AO, Tamagnan G, Kimes AS, Chambers J, Vaupel DB, King SL, Picciotto MR, Innis RB and London ED (2000) 5-Iodo-A-85380, an $\alpha 4\beta 2$ subtype-selective ligand for nicotinic acetylcholine receptors. *Mol Pharmacol* **57**:642-649.

Nelson ME, Kuryatov A, Choi CH, Zhou Y and Lindstrom J (2003) Alternate stoichiometries of $\alpha 4\beta 2$ nicotinic acetylcholine receptors. *Mol Pharmacol* **63**:332-341.

Picciotto MR, Zoli M, Lena C, Bessis A, Lallemant Y, LeNovere N, Vincent P, Pich E, Bruret P, Changeux J-P (1995) Abnormal avoidance learning in mice lacking functional high-affinity nicotine receptor in the brain. *Nature* **374**:65-67.

Ross SA, Wong JY, Clifford JJ, Kinsella A, Massalas JS, Horne MK, Scheffer IE, Kola I, Waddington JL, Berkovic SF, Drago J (2000) Phenotypic characterization of an $\alpha 4$ neuronal nicotinic acetylcholine receptor subunit knock-out mouse. *J Neurosci* **20**:6431-6441.

Salminen O, Murphy KL, McIntosh JM, Drago J, Marks MJ, Collins AC, Grady SR (2004) Subunit composition and pharmacology of two classes of striatal presynaptic nicotinic acetylcholine receptors mediating dopamine release in mice. *Mol Pharmacol* **65**:1526-1535.

Tapia L, Kuryatov A and Lindstrom J (2007) Ca^{2+} permeability of the $(\alpha 4)_3(\beta 2)_2$ stoichiometry greatly exceeds that of $(\alpha 4)_2(\beta 2)_3$ human acetylcholine receptors. *Mol Pharmacol* **71**(3):769-776.

Mol 45203

Vailati S, Hanke W, Bejan A, Barabino B, Longhi R, Balestra B, Moretti M, Clementi F and Gotti C

(1999) Functional $\alpha 6$ -containing nicotinic receptors are present in chick retina. *Mol Pharmacol* **56**:11-19.

Whiteaker P, Marks MJ, Grady SR, Lu Y, Picciotto MR, Changeux JP, Collins AC (2000b)

Pharmacological and null mutation approaches reveal nicotinic receptor diversity. *Eur J Pharmacol* **393**:123-135.

Whiteaker P, Cooper JF, Salminen O, Marks MJ, McClure-Begley TM, Brown RWB, Collins AC and

Lindstrom JM (2006) Immunolabeling demonstrates the interdependence of mouse brain $\alpha 4$ and $\beta 2$ nicotinic acetylcholine receptor subunit expression. *J Comp Neurol* **499**:1016-1038.

Whiting P, Lindstrom J (1988) Characterization of bovine and human neuronal nicotinic acetylcholine receptors using monoclonal antibodies. *J Neurosci* **8**:3395-3404.

Zhou Y, Nelson ME, Kuryatov A, Choi C, Cooper J, Lindstrom J. (2003) Human $\alpha 4 \beta 2$ acetylcholine receptors formed from linked subunits. *J Neurosci* **23**:9004-9015.

Zoli M, Lena C, Picciotto MR, Changeux J-P. (1998) Identification of four classes of nicotinic receptors using beta2 mutant mice. *J Neurosci* **18**:4461-4472.

Zoli M, Moretti M, Zanardi A, McIntosh JM, Clementi F and Gotti C (2002) Identification of the nicotinic receptor subtypes expressed on dopaminergic terminals in the rat striatum. *J Neurosci* **22**:8785-8789.

Zwart R, Vijverberg HP (1998) Four pharmacologically distinct subtypes of $\alpha 4 \beta 2$ nicotinic acetylcholine receptor expressed in *Xenopus laevis* oocytes. *Mol Pharmacol* **54**:1124-1131.

Mol 45203

Footnotes:

This work was supported by research grant DA003194 and animal resources grant DA015663 from the National Institute of Drug Abuse to A. C. Collins and by the Fondazione Cariplo grant n° 2006/0882/104878 to F. Clementi and Fondazione Cariplo grant n° 2006/0779/109251 and FP7-Health-2007A grant n°202088-NeuroCypres from the EC to C.Gotti.

LEGENDS TO FIGURES

Figure 1.

[¹²⁵I]-A85380 binding in membranes prepared from cortical and thalamic synaptosomes.

Saturation curves for ¹²⁵I-A85380 binding were constructed using membranes prepared from cortical (Panel A, $\alpha 4$ mice; Panel B, $\beta 2$ mice), or thalamic (Panel C, $\alpha 4$ mice; Panel D, $\beta 2$ mice) synaptosomes remaining after the measurement of functional responses. The effects of sequential $\alpha 4$ and $\beta 2$ gene deletion on maximal [¹²⁵I]-A85380 binding in cortex (Panel E) and thalamus (Panel F) are compared. Values represent mean \pm SEM of 4 separate determinations.

Figure 2.

ACh stimulation of ⁸⁶Rb⁺ efflux from cortical synaptosomes.

Crude cortical synaptosomes were prepared from cerebral cortex of $\alpha 4^{+/+}$ (Panel A, n=15), $\alpha 4^{+/-}$ (Panel B, n=18), $\alpha 4^{-/-}$ (Panel C, n=6), $\beta 2^{+/+}$ (Panel D, n=13), $\beta 2^{+/-}$ (Panel E, n=16) and $\beta 2^{-/-}$ (Panel F, n=4) mice. ⁸⁶Rb⁺ efflux was measured using the indicated [acetylcholine] as described in the Methods. Data were fit to a two component model and the results of these curve fits are shown with the solid line. Higher and lower sensitivity components are indicated by the dashed and dotted lines, respectively. The effects of $\alpha 4$ or $\beta 2$ gene deletion on the maximal higher ACh sensitivity and lower ACh sensitivity components of ⁸⁶Rb⁺ efflux are shown in panels G and H, respectively. A significant difference ($P < 0.05$) between $\alpha 4^{+/-}$ and $\beta 2^{+/-}$ is indicated by the asterisk (*) in Panel H.

Figure 3.

ACh stimulation of $^{86}\text{Rb}^+$ efflux from thalamic synaptosomes.

Crude synaptosomes were prepared from thalamus of $\alpha 4^{+/+}$ (Panel A, n=15), $\alpha 4^{+/-}$ (Panel B, n=18), $\alpha 4^{-/-}$ (Panel C, n=6), $\beta 2^{+/+}$ (Panel D, n=13), $\beta 2^{+/-}$ (Panel E, n=16) and $\beta 2^{-/-}$ (Panel F, n=4) mice. $^{86}\text{Rb}^+$ efflux was measured using the indicated [Acetylcholine] as described in the Methods. Data were fit to a two component model and the results of these curve fits are shown with the solid line. Higher and lower sensitivity components are indicated by the dashed and dotted lines, respectively. The effects of $\alpha 4$ or $\beta 2$ gene deletion on the maximal higher ACh sensitivity and lower ACh sensitivity components of $^{86}\text{Rb}^+$ efflux are shown in panels G and H, respectively. A significant difference ($p < 0.05$) or ($p < 0.01$) between $\alpha 4^{+/-}$ and $\beta 2^{+/-}$ mice are indicated with a single (*) or double (**) asterisk, respectively..

Figure 4

Immunoprecipitation analysis of the subunit content of the nAChRs labelled with 2nM [^3H]-epibatidine, expressed in the cortex (A) and thalamus (B) of the $\alpha 4^{+/+}$, $\alpha 4^{+/-}$, $\alpha 4^{-/-}$, $\beta 2^{+/+}$, $\beta 2^{+/-}$, $\beta 2^{-/-}$ genotypes

Immunoprecipitation was carried out as described in Materials and Methods using saturating concentrations (20-30 μg) of anti-subunit Abs. The amount immunoprecipitated by each antibody was subtracted from the value obtained in control samples containing an identical concentration of normal rabbit IgG. The results obtained with each Ab are expressed as fmol of immunoprecipitated [^3H]-epibatidine labeled nAChR / mg of protein. The results are the mean values \pm SEM of three experiments performed in duplicate for the cortex (A) and, two experiments performed in triplicate for each antibody for the thalamus (B). The statistical

Mol 45203

analyses were made using Student's paired *t* test. The significance of the differences from controls were * $p < 0.05$; ** $p < 0.01$; *** $p < 0.001$.

Figure 5

Sucrose gradient analysis of cortical $\alpha 4^{+/+}$, $\alpha 4^{-/-}$ $\beta 2^{+/+}$, $\beta 2^{-/-}$ genotypes.

500 μ l of 2% Triton X-100 extracts from each genotype were loaded onto a 5-20% (wt / vol) sucrose gradient in phosphate buffer saline pH 7.5, 0.1% Triton X-100 and 1 mM PMFS, and centrifuged for 14 hours at 40000 rpm in a Beckman rotor at 4°C as described in Materials and Methods. The fractions were collected, added to anti- $\alpha 4$ or $\beta 2$ Abs bound to microwells, left for 24 hours, and then assayed for ^3H -Epi binding as described in Materials and Methods. As a standard [^{125}I]- α Bgtx labeled Torpedo AChR were subjected to sucrose gradient centrifugation in parallel, the fractions were collected and the radioactivity determined by γ counting and shown are the peaks of monomer (9S) and dimer (11.5) Torpedo AChR.

Figure 6

Western blot analysis of antibody specificity in cortical extracts (A) and purified $\alpha 4\beta 2^*$ receptors from mouse cortex (B)

A) The samples obtained from the $\alpha 4^{+/+}$, $\alpha 4^{-/-}$ $\beta 2^{+/+}$ and $\beta 2^{-/-}$ genotypes were prepared as described in Materials and Methods. The proteins were separated on 9% acrylamide SDS gels, electrotransferred to nitrocellulose, probed with 1-2.5 μ g/ml of the indicated primary Abs, and then incubated with the secondary Ab (anti-rabbit conjugated to peroxidase, dilution 1:40000). The bound Abs were revealed by a chemiluminescent substrate (Pierce, Rockford, IL, USA)

Mol 45203

The anti- $\alpha 4$ Ab recognised a band of 68-70 kDa (corresponding to the expected size of the $\alpha 4$ subunit) in the wild-type but not in the null mutant mice, and the anti- $\beta 2$ Ab recognized a band of 52kDa (corresponding to the expected size of the $\beta 2$ subunit) in the wild-type but not in the null mutant mice.

The molecular weight markers (top to bottom) are 97 kDa, 66 kDa and 45 kDa, 31 kDa.

B) The $\beta 2^*$ receptors were purified as described in Materials and Methods. The proteins were concentrated and then separated on 9% acrylamide SDS gels, electrotransferred to nitrocellulose, probed with 1-2.5 $\mu\text{g/ml}$ of the indicated Abs, and processed as described above.

Figure 7

Analysis of $\alpha 4$ and $\beta 2$ subunit content in cortical nAChRs prepared after gradient separation of the different genotypes.

A) Western blot analysis of 10 μg of the concentrated fractions of the sucrose gradients from one representative experiment involving all genotype, tested for the presence of $\alpha 4$ and $\beta 2$ subunits. The proteins were separated on 9% acrylamide SDS gels, electrotransferred to nitrocellulose, and processed as described in Figure 6.

B)_Optical density ratios of the $\alpha 4$ and $\beta 2$ subunits in the different genotypes

These ratios are the mean values \pm SEM of the Western blots of four separate experiments for each cortex genotype. The optical density ratio was calculated taking the optical density of the wild-type as 1.

The normalized optical density ratios of $\alpha 4$ and $\beta 2$ subunits in $\alpha 4^{+/-}$ and $\beta 2^{+/-}$ were significantly different (Mann-Whitney test $*P = 0.038$ and $***P = 0.0004$ respectively).

Mol 45203

Figure 8

Optical density ratios of the $\alpha 4$ and $\beta 2$ subunits in sucrose gradient fractions of cortex from the $\alpha 4^{+/+}$, and $\alpha 4^{+/-}$, and the $\beta 2^{+/+}$ and $\beta 2^{+/-}$ genotypes .

A) A total of 2 or 1 fmol of $\alpha 4^{+/+}$ (lanes 1 and 2) or $\alpha 4^{+/-}$ (lanes 3 and 4) of [^3H]-epibatidine binding sites were loaded per lane. The samples were separated on 9% acrylamide SDS gels, electrotransferred to nitrocellulose, and processed as described in Figure 6.

The same blots were first incubated with anti- $\alpha 4$ Abs, and then stripped and incubated with anti- $\beta 2$ Abs or vice versa.

The developed films were acquired as described in Materials and Methods and the images were analyzed using NIH Image J software (National Technical Information Service, Springfield, VA,USA). The pixel values of all of the images were transformed to optical density values by the program using the calibrated curve obtained by acquiring the calibrated tablet using the same parameters as those used for the images.

The ratios between the optical densities of lane 3 and lane 1, and lane 4 and lane 2, were obtained for both $\alpha 4$ and $\beta 2$ Abs.

B) Mean values \pm SEM of optical density ratios of the $\alpha 4$ and $\beta 2$ subunits in the $\alpha 4$ (left) $\beta 2$ genotypes (right) of heterozygote/wild type mice in the $\alpha 4$ genotype (left) and $\beta 2$ genotypes (right) obtained from four separate genotype experiments.

The cortex $\alpha 4$ and $\beta 2$ subunit ratios in the $\alpha 4^{+/-}/\alpha 4^{+/+}$ and $\beta 2^{+/-}/\beta 2^{+/+}$ genotypes were statistically significant (Mann-Whitney test $**P=0.0022$ for both).

Figure 9

Mol 45203

Analysis of $\alpha 4$ and $\beta 2$ subunit content in thalamic nAChRs prepared after gradient separation of the different genotypes.

A) Western blot analysis of 7 μ g of the concentrated sucrose density gradient fractions from one representative experiment involving all genotypes, and tested for the presence of $\alpha 4$ and $\beta 2$ subunits.

The proteins were separated on 9% acrylamide SDS gels, electrotransferred to nitrocellulose, and processed as described in Figure 6.

B)_Optical density ratios of the $\alpha 4$ and $\beta 2$ subunits in the different genotypes

These ratios are the mean \pm SEM of Western blots of three separate experiments for each genotype. The optical density ratio was calculated by taking the optical density of the wild-type as 1.

The normalized optical density ratios of the $\alpha 4$ and $\beta 2$ subunits were not statistically significant (ns) in the $\alpha 4^{+/-}$ mice, but $\beta 2^{+/-}$ significantly different in the $\beta 2^{+/-}$ mice (Mann-Whitney test (*P =0.015)

Figure 10

Optical density ratios of the $\alpha 4$ and $\beta 2$ subunits in sucrose gradient fractions of thalamus from the $\alpha 4^{+/+}$ and $\alpha 4^{+/-}$ and the $\beta 2^{+/+}$ and $\beta 2^{+/-}$ genotypes.

A) A total of 2 or 1 fmol of [3 H]-epibatidine binding sites for $\alpha 4^{+/+}$ (lanes 1 and 2) or $\alpha 4^{+/-}$ (lanes 3 and 4) binding sites were loaded per lane. The samples were separated on 9% acrylamide SDS gels, electrotransferred to nitrocellulose, and processed as described in Figure 8

Mol 45203

The same blots were first incubated with anti- $\alpha 4$ Abs, and then stripped and incubated with anti- $\beta 2$ Abs or vice versa. The samples were processed, analyzed and expressed as described in Figure 8A

B) Mean values \pm SEM of optical density ratios of the $\alpha 4$ and $\beta 2$ subunits in the $\alpha 4$ (left) and $\beta 2$ genotypes (right) of heterozygote/wild-type obtained from three separate genotype experiments.

The thalamic heterozygote/wild-type $\alpha 4$ and $\beta 2$ subunit ratios were statistically significant in the $\alpha 4^{+/-}/\alpha 4^{+/+}$ and $\beta 2^{+/-}/\beta 2^{+/+}$ genotypes (Mann-Whitney test * $P=0.029$ and ** $P=0.0079$ respectively).

Mol 45203

Table 1 Specific activities of the membrane, 2% Triton extracts and concentrated gradient fractions

CORTEX	$\alpha 4^{+/+}$	$\alpha 4^{+/-}$	$\alpha 4^{-/-}$	$\beta 2^{+/+}$	$\beta 2^{+/-}$	$\beta 2^{-/-}$
Membrane	64.9±7.2	33.9±3.3	2.5±1.3	76.4 ± 3.9	41.4 ± 2.7	2.0 ± 1.7
2% Triton X-100	66.7±10.6	34.6±1.6	3.1±0.8	76.5±14.2	37.7±4.6	1.1±0.1
Concentrated Gradient Fraction	222±32.8	116±17.1	12.1±3.9	247.5±21.3	123.8±12.3	2.4±2.0

THALAMUS	$\alpha 4^{+/+}$	$\alpha 4^{+/-}$	$\alpha 4^{-/-}$	$\beta 2^{+/+}$	$\beta 2^{+/-}$	$\beta 2^{-/-}$
Membrane	187.8±23.8	105.0±20.3	18.5±9.2	177.4±10.6,	106.4± 15.2	10.0± 3.4
2% Triton X-100	149.5±26.5	89.9±19.9	11.8±4.0	170.3±27.3	90.5±2.3	9.5±5.5
Concentrated Gradient Fraction	227.1±30.5	138.8±13.1	25.75±2.3	288.6±21,9 4	185.4±17.2	22.3±1.3

Values are expressed as fmol/mg of protein and are the mean ±SEM of 4-6 separate experiments for the cortex and 3 separate experiments for the thalamus.

Figure 1.

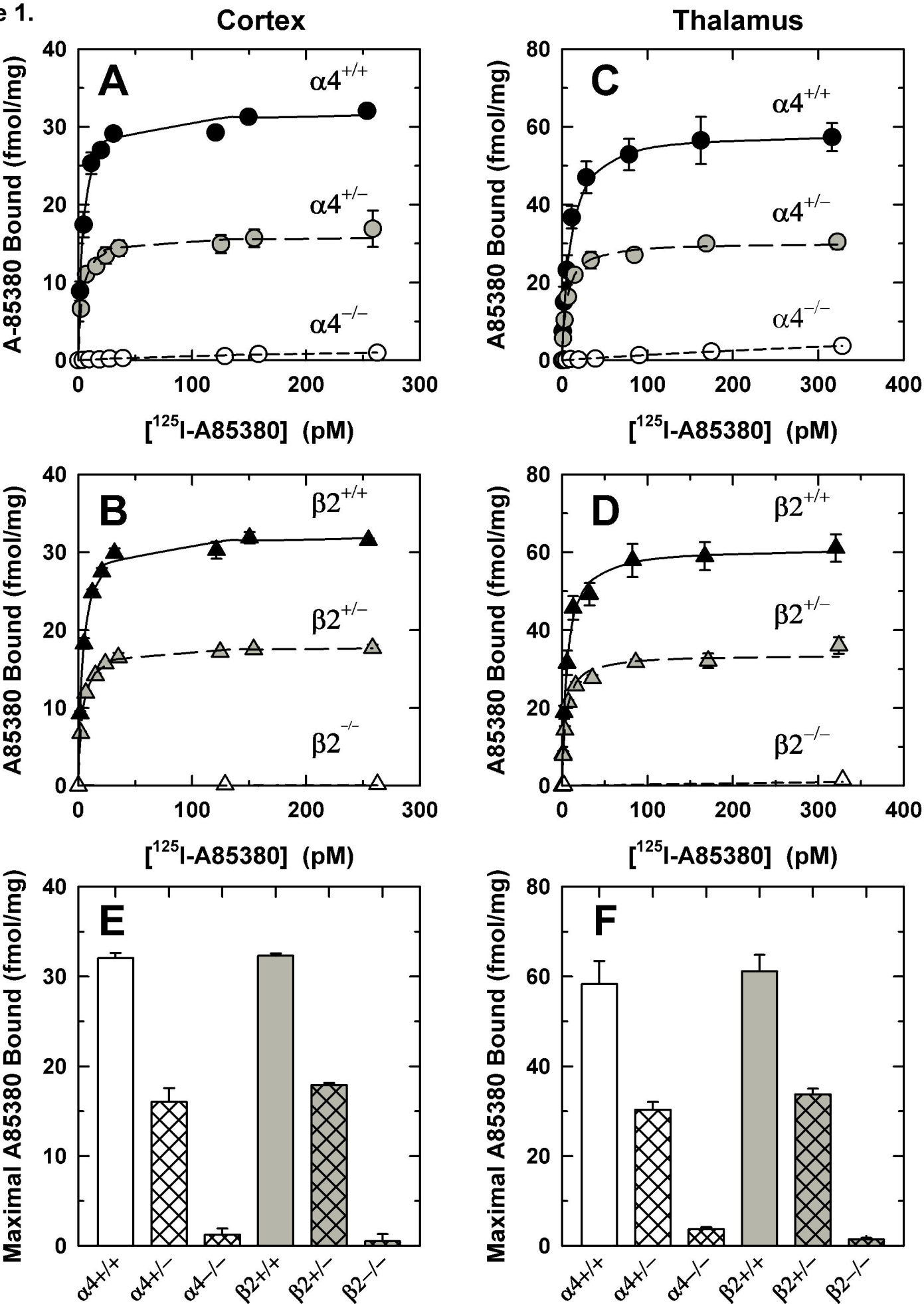


Figure 2.

CORTEX

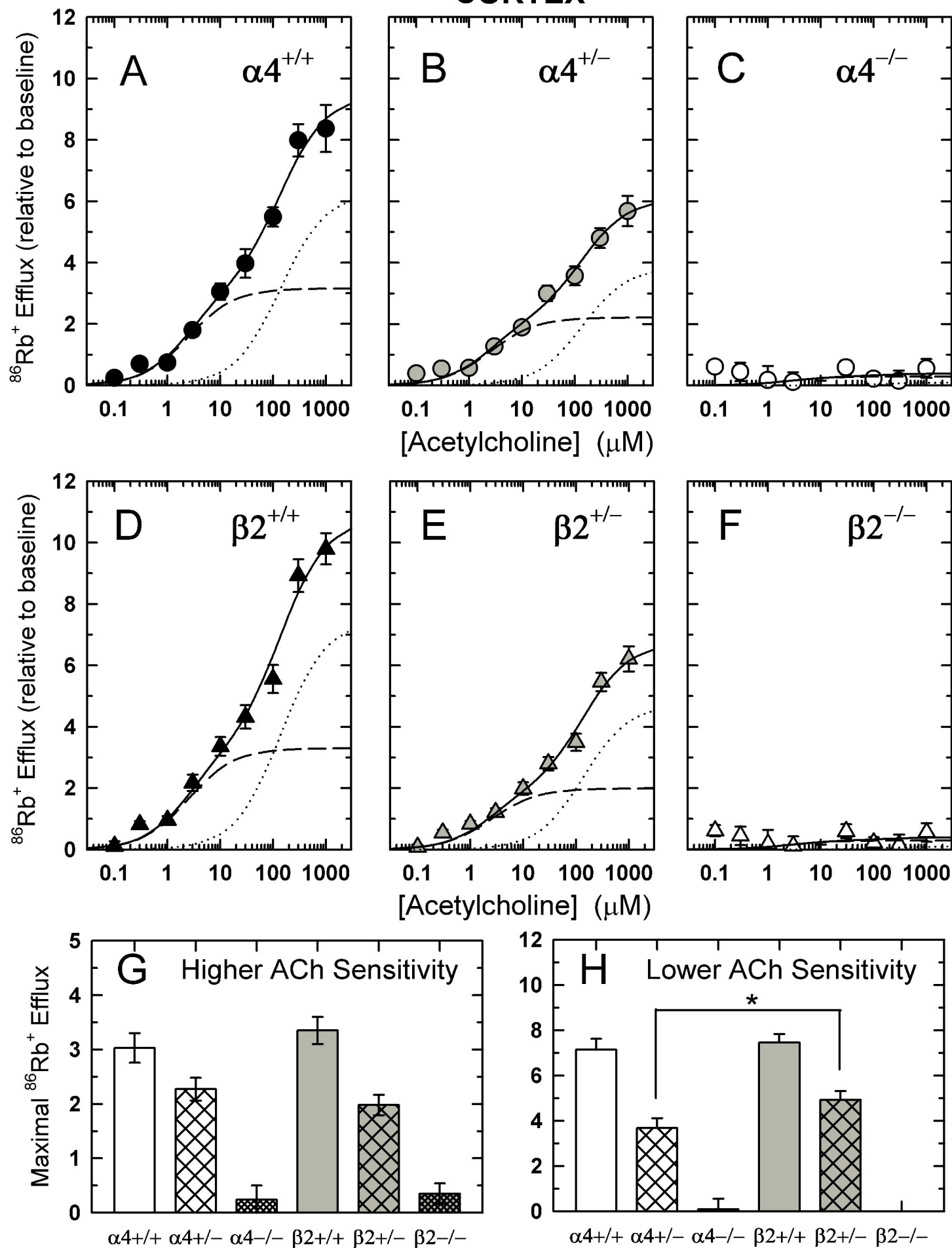


Figure 3.

THALAMUS

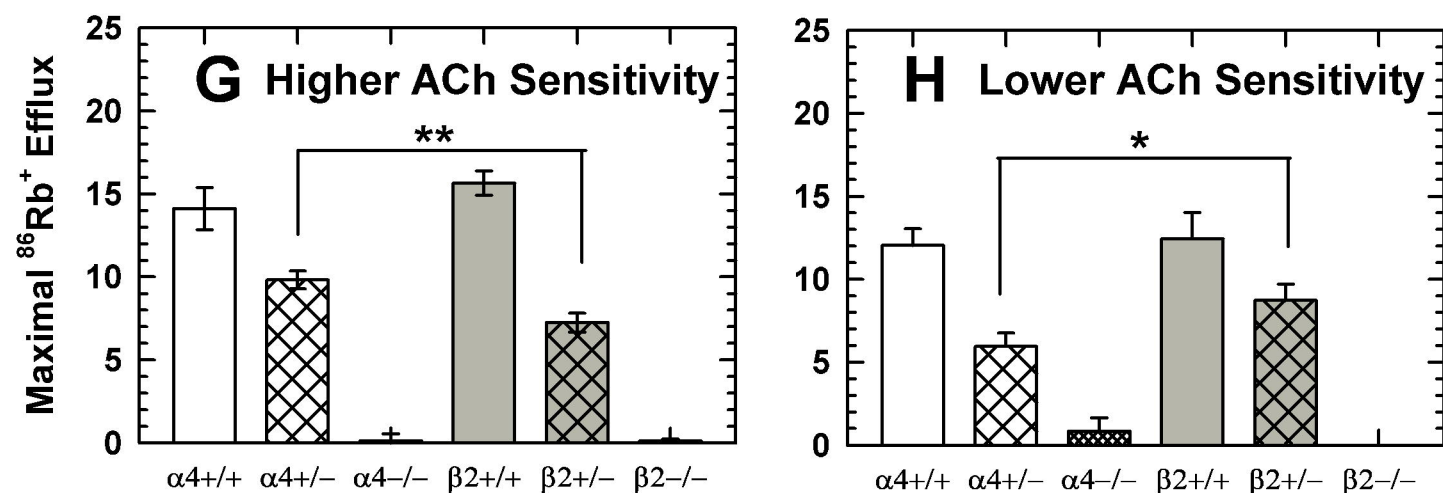
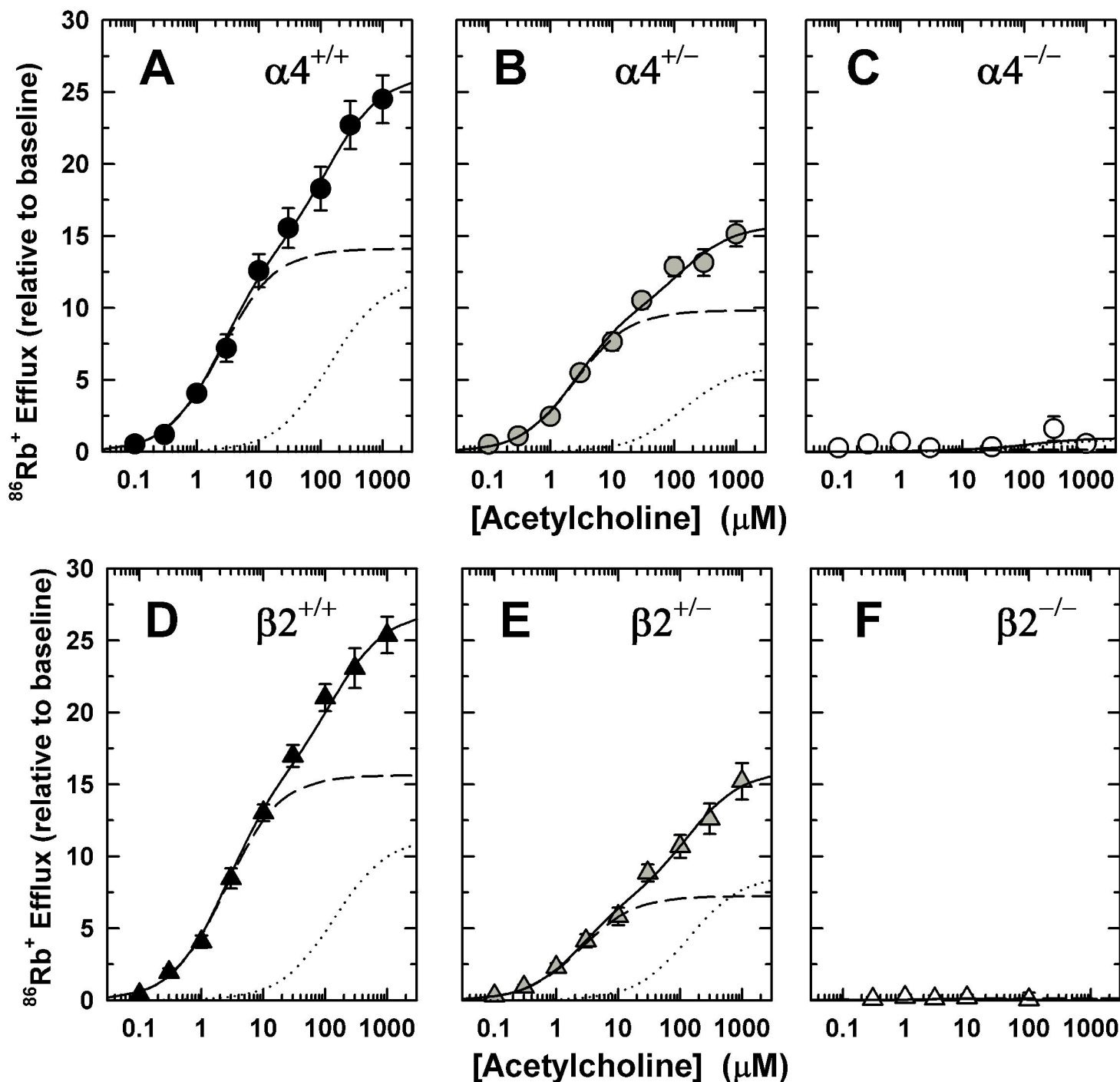


Figure 4

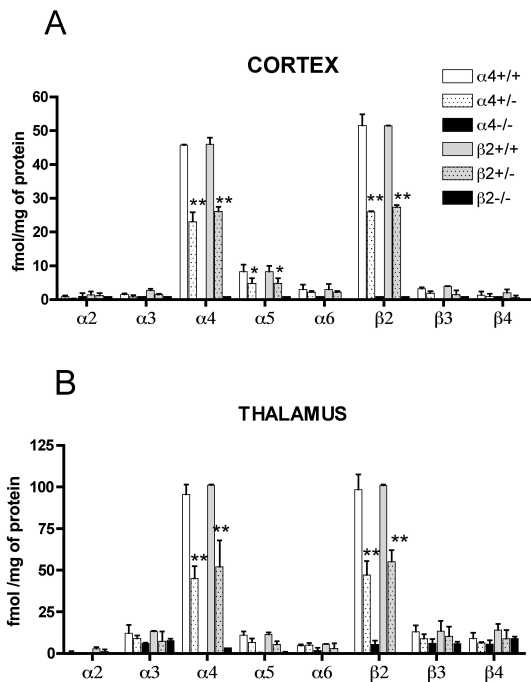
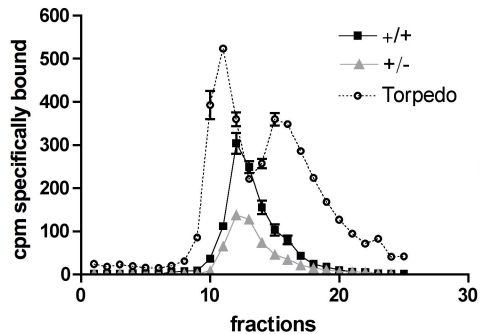


Figure 5

$\alpha 4$ genotype



$\beta 2$ genotype

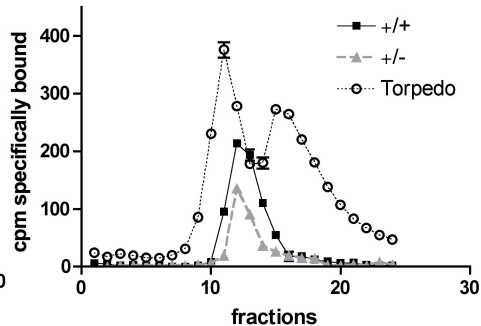
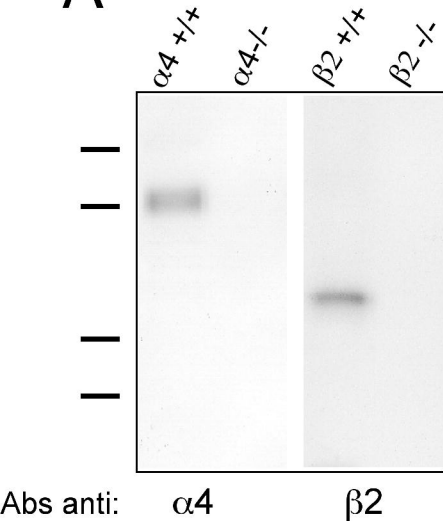


Figure 6

A



B

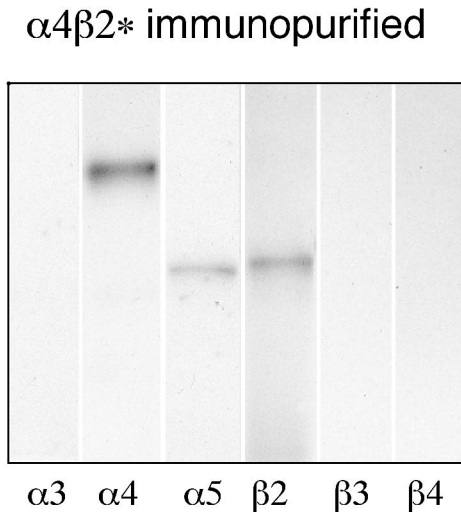
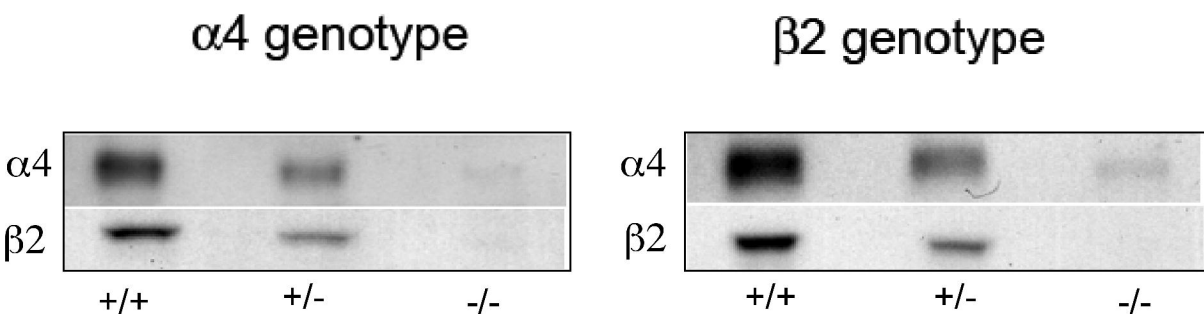


Figure 7

CORTEX

A



B

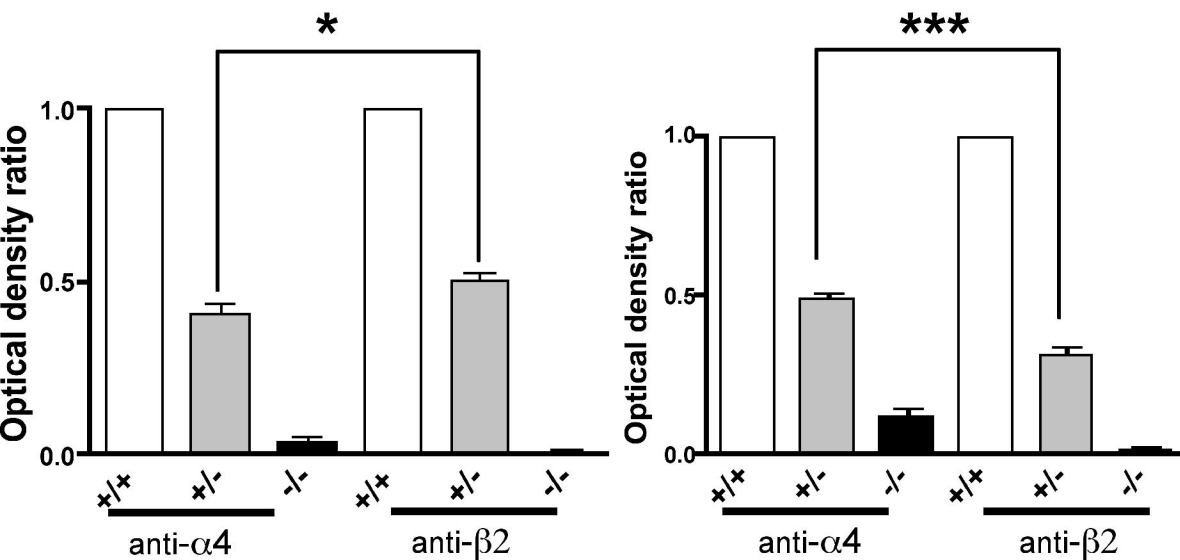


Figure 8

CORTEX

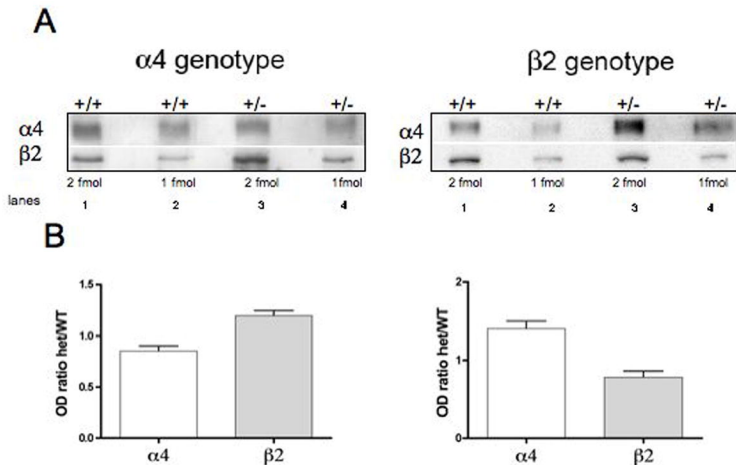
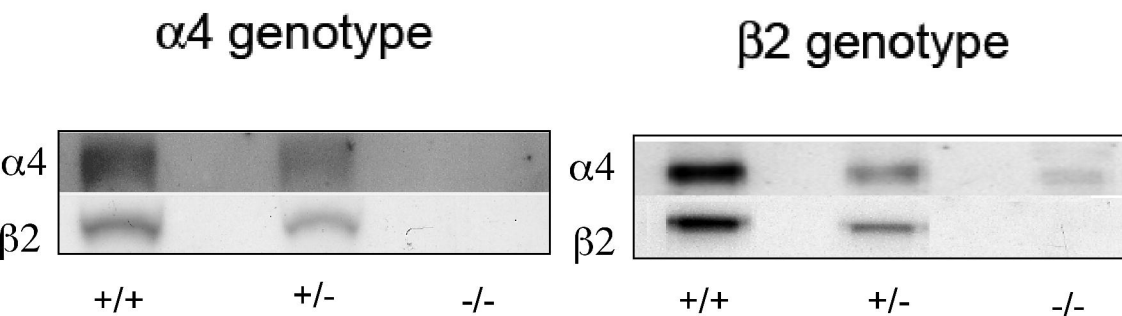


Figure 9

THALAMUS

A



B

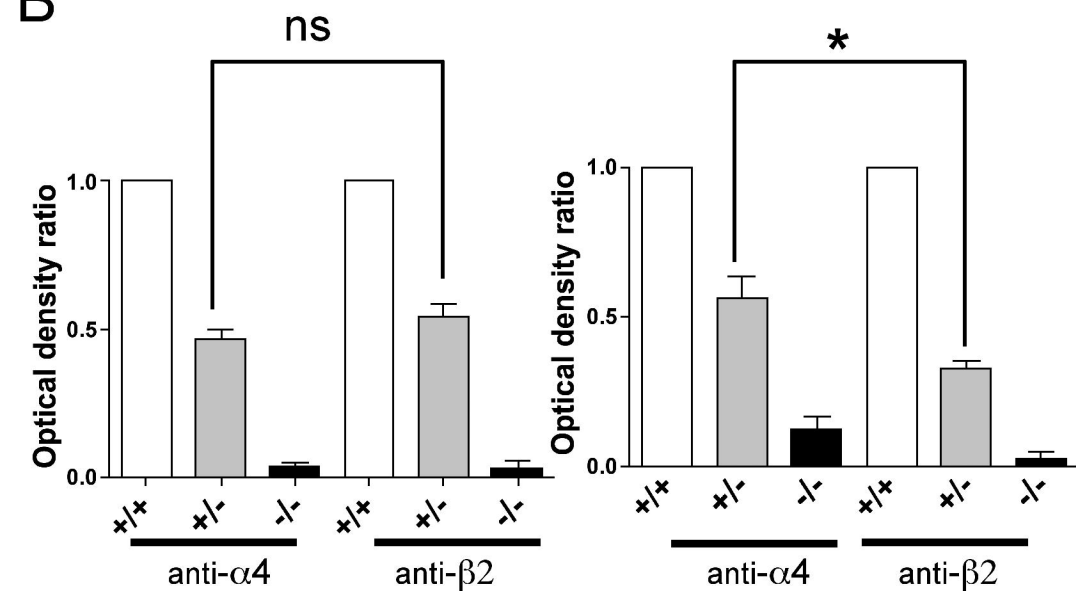


Figure 10

THALAMUS

